Short-Packet Amplify-and-Forward Relaying for the Internet-of-Things in the Face of Imperfect Channel Estimation and Hardware Impairments

Vahid Shahiri, Ali Kuhestani, *Member, IEEE* and Lajos Hanzo, *Fellow, IEEE*

Invited Paper

.

***Abstract*—In next-generation wireless systems ultra-reliable low-latency communications (URLLC) have to be realized in support of the Internet-of-things (IoT). However, this is quite a challenge in the face of channel estimation errors (CEEs) and hardware imperfections (HWIs). Hence, we consider a variety of realistic HWIs as well as CEEs and evaluate the average block error rate (BLER) of a short-packet based cooperative amplify-and-forward (AF) relaying network. Our simulation and analytical results reveal that as expected, both the CEEs and HWIs lead to a substantial average BLER degradation. In particular, CEEs lead to a BLER floor, which is further aggravated by the increase in HWIs. A high level of HWIs results in a BLER tending to one, regardless of the transmit power. Furthermore, it is shown that the CEEs and HWIs gravely degrade the energy efficiency of the idealized perfect scenario. This observation shows that both the CEEs and HWIs constitute critical issues in the design of energy efficient communication systems. However, through solving the optimization problems formulated, we conceived several schemes for mitigating the degradations imposed by the CEEs and HWIs. e.g. in our adaptive-duration training scheme the total CEE of the hops is shared in line with the current status of the two channels. Our simulation results show that this scheme significantly reduces the BLER and mitigates the deleterious effects of CEE.**

***Index Terms*: Finite block-length regime, Cooperative AF relaying, Imperfect CSI, Hardware imperfection.**

I. Introduction

In addition to the so-called Enhanced Mobile Broad Band (eMBB) mode, the fifth-generation (5G) cellular system is expected to support both machine-to-machine (M2M) communications and internet-of-things (IoT) [1], [2]. In some IoT applications such as Industrial IoT (IIoT), having a low latency is vital for guaranteeing real-time communications [3]. Additionally, applications like remote surgery and autonomous vehicles cannot tolerate a latency higher than 250 μs [4], hence packets of extremely short lengths are needed. However, short-packet communication (SPC) introduces unique challenges in wireless applications. Classic Shannon theory is only applicable to long packets, hence providing inaccurate estimate of the maximum achievable rate in short-packet scenarios. Motivated by this Polyanskiy *et al.*, [5] investigated the maximum achievable channel coding rate at a given finite block-length and error probability. Based on this, an error probability bound was then derived for a given block-length and coding rate. These results led to a new theoretical framework for analyzing SPCs. Furthermore, Polyanskiy *et al.* [5] presented a modification to the method of analyzing cooperative scenarios on the basis of classic Shannon theory.

Very recently, the performance of SPC has also been examined in various wireless communication scenarios [6]-[13]. By assuming a generalized Nakagami-m fading channel, the authors of [6] have studied a short-packet based non-orthogonal multiple access (NOMA) IoT network relying on partial channel state information (CSI). A pair of IoT networks - namely a terrestrial and and aerial network - are investigated and asymptotic as well as exact coverage probability are derived. In [7], the authors investigated both the maximal rate achievable for a given block-length as well as the error probability for transmission over quasi-static multiple-input multiple-output (MIMO) fading channels. In [8], an optimal transmission strategy is designed for maximizing the average achievable data rate of a multiple-input single-output (MISO) SPC system. The authors of [9]-[11] have investigated SPC in one-way relaying scenarios. Sum-block error rate (BLER) performance of two-way amplify-and-forward (AF) relaying is derived in [12], and an asymptotic expression is obtained for the sum-BLER at asymptotically high signal-to-noise ratios (SNR). In [13], hybrid automatic repeat request (HARQ) assisted decode-and-forward (DF) relaying is investigated in the context of Nakagami-m fading channels, while selection combining (SC) and maximum ratio combining (MRC) is employed at the receiver.

In practical communication systems, all nodes exhibit hardware-related imperfections, such as phase noise, I/Q imbalance, non-ideal filters, non-linear power amplifiers, etc. [14]-[19]. The deleterious effects of hardware impairments (HWIs) become more significant, when employing inexpensive hardware. As a result, this effect is expected to be particularly

V. Shahiri is with the Electrical Engineering Department, Amirkabir University of Technology, Tehran, Iran (e-mail: shahirivahid@aut.ac.ir).

A. Kuhestani is with the Communications and Electronics Department, Faculty of Electrical and Computer Engineering, Qom University of Technology (QUT), Qom 3716146611, Iran (e-mail: kuhestani@qut.ac.ir, corresponding author).

L. Hanzo is with the School of Electronics and Computer Science, University of Southampton, Southampton SO17 1BJ, U.K. (e-mail: lh@ecs.soton.ac.uk).

L. Hanzo would like to acknowledge the financial support of the Engineering and Physical Sciences Research Council projects EP/P034284/1 and EP/P003990/1 (COALESCE) as well as of the European Research Council's Advanced Fellow Grant QuantCom (Grant No. 789028)

pronounced in the IoT and in wireless sensor networks (WSN) relying on low-cost hardware [17]-[19]. The effect of HWIs can be alleviated by a sophisticated blend of analogue and digital signal processing techniques [15], although they cannot completely eliminate these imperfections. According to [15], the remaining HWIs can be modeled as an additive distortion and the experimental results of [16] reveal the accuracy of the proposed model. Against this background, this is the first contribution that examines the effect of HWIs in SPC systems.

To elaborate a little further, most of the papers related to SPC have assumed that perfect channel state information (CSI) is available at the receiver. However, in practical systems, this is an over-optimistic assumption. Explicitly, due to realistic factors such as the feedback delay, limited training power and duration, limited feedback rate [20], unexpected user mobility, channel fading variations [21] tend to impair the channel estimation process. Very recently, some authors have studied the impact of CEEs in short-packet scenarios [21]-[24]. In [21], the outage probability of a multi-user MIMO (MU-MIMO) aided SPC system considering CEE is studied. The CEEs in [21] are treated as signals rather than interference and noise. The authors of [22] have characterized the trade-off between the training sequence length and information codeword length. The results of [22] show that the optimized training sequence length and rate adaptation strategy reduces the delay violation probability, compared to conventional strategies that do not consider the delay constraints. Moreover the authors of [23] have maximized the finite block-length throughput of a two-hop DF relaying system under outdated CSI. As a further advance, the authors of [24] have studied the emerging MU-MIMO concept in a short-packet aided IoT network under shadow fading, assuming both perfect and imperfect CSI. We remark that none of the above-mentioned treatises have studied the BLER performance of SPCs in an AF relaying scenario in the presence of CEEs.

In contrast to most of the papers on cooperative SPCs, which have considered DF relays [9]-[11], [13], in this contribution, we investigate the average BLER of SPC systems in a two-hop AF relaying network, where all the nodes suffer from HWIs and the channel estimation process of both hops is subject to estimation error. Considering AF relays while assuming imperfect hardware and CEE makes our analysis mathematically challenging compared to the state-of-the-art. Furthermore, we generalize the system model of [12] where both the hardware and the channel estimation are considered to be perfect. The main contributions of this paper are boldly and explicitly contrasted to the literature in Table 1 and are summarized as follows:

- We first calculate the received instantaneous signal-to-noise-plus-distortion-ratio (SNDR) for our scenario both at the relay node (RN) and at the destination node (DN). Based on this, a novel closed-form expression is derived for the outage probability (OP) when the channel coefficients in both hops follow the Nakagami-m distribution.
- New exact closed-form expressions are derived for the average BLER of two special cases, namely imperfect hardware in the presence of perfect CSI and imperfect estimation relying on perfect hardware for transmission over Rayleigh channels. Then using the classic Riemannian approximation, simple closed-form expressions are extracted for the general scenario of Nakgami-m and Rayleigh fading channels. Our simulation results show that using this approximation provides very accurate results even for low number of channel uses, while considerably simplifying our expressions.
- To provide practical insights, we have analyzed our system model in the asymptotically high-SNR regime. The resultant high-SNR expressions show that while the CEE is the dominant source of the error floor, the presence of significant HWIs will lead to substantial error-floor. This observation highlights the benefit of having a low level of CEE. Moreover, using the high-SNR expressions, a pair of optimization problems is formulated with the aim of minimizing the average BLER by allocating the optimum power and by the efficient distribution of the tolerable HWIs.
- To glean further insights concerning both the imperfect hardware with perfect channel estimation and the erroneous estimation scenario relying on perfect hardware, we have analyzed the average BLER in the asymptotically high SNR scenario. In the latter case an adaptive training scheme is proposed for the most beneficial sharing of the total tolerable CEE of the system between the two hops. Our simulation results show that while the presence of CEE in our SPC scenario can significantly degrade the system performance, the proposed scheme substantially reduces the average BLER by mitigating the effect of CEEs.
- We have also presented a detailed discussion on the energy efficiency aspects of the proposed system model, which is vitally important in the design of energy-efficient systems. The results show that both the CEE and HWI severely degrade the energy efficiency of cooperative SPC schemes. In our future work, we plan to tackle the energy efficiency issues of SPC systems using Pareto optimization techniques [25].

The symbols used in this paper are listed in Table II. The remainder of this paper is organized as follows. In Section II, we introduce our system model and the main parameters used. In Section III, the general average BLER problem is formulated and an approximate expression based on Riemannian approximation is presented for a Nakagami-m fading channel. The exact closed-form expression of the average BLER is derived both for the perfect CSI and perfect hardware scenarios in Section IV for a Rayleigh channel. To gain some practical insights, in Section V our complex expressions are tightly approximated for the asymptotic and high SNR regimes. In Section VI, by using the high SNR expressions in the previous section, the average BLER is minimized by beneficially distributing the tolerable HWI and CEE with the aid of optimal power allocation between the source and relay. Our numeric results are presented in Section VII, while our conclusions are offered in Section VIII.

TABLE I: Contrasting our contributions to the state-of-the art

Contributions	**This work**	[8]	[11]	[12]	[21]	[22]	[23]	[24]
Cooperation	✓		✓	✓			✓	
Imperfect CSI	✓	✓			✓	✓	✓	✓
Imperfect HW	✓							

TABLE II: List of symbols

Symbol	**Description**	**Symbol**	**Description**
P_S	Power of source node	P_R	Power of relay node
h_{SR}	Channel coefficient of source-relay link	h_{RD}	Channel coefficient of relay-destination link
$\hat{h}_{SR}$	Estimated channel of source-relay link	$\hat{h}_{RD}$	Estimated channel of relay-destination link
η_S^t	Impairment term of transmitter	η_D^r	Impairment term of receiver
η_R^r	Impairment term of relay in receiving	η_R^t	Impairment term of relay in transmitting
n_R	Noise term in relay	n_D	Noise term in destination
$\sigma^2_{e_{SR}}$	Channel estimation error in source-relay link	$\sigma^2_{e_{RD}}$	Channel estimation error in relay-destination link
k_S^t	Impairment factor of source node	k_D^r	Impairment factor of destination node
k_R^r	Impairment factor of relay in receiving	k_R^t	Impairment factor of relay in transmitting
m_1	Shape parameter of Nakagami-m distribution in source-relay link	m_2	Shape parameter of Nakagami-m distribution in relay-destination link
θ_1	Scale parameter of Nakagami-m distribution in source-relay link	θ_2	Scale parameter of Nakagami-m distribution in relay-destination link
β_1	Channel parameter of Rayleigh distribution in source-relay link	β_2	Channel parameter of Rayleigh distribution in relay-destination link
m	Duration of each time slot quantified in terms of channel uses	$\hat{m}$	Number of channel uses in each packet transmission
ϵ	Block error rate	N_0	Thermal noise power

II. System Model

We consider a one-way relaying network consisting of a source node, $\mathcal{S}$, relay node, $\mathcal{R}$, and destination node, $\mathcal{D}$. All the nodes considered in our scenario are single-antenna aided half-duplex devices. Our assumption is that there is no direct link between the source and destination due to obstacles or severe attenuation. The $\mathcal{S}$-$\mathcal{R}$ and $\mathcal{R}$-$\mathcal{D}$ links suffer from Rayleigh fading. We assume quasi-static fading, for which the channel coefficients remain constant during each transmission block and change independently from one block to the other. Without loss of generality, we assume that the thermal noise at the nodes ($\mathcal{S}$, $\mathcal{R}$, and $\mathcal{D}$), obey the white Gaussian distribution $\mathcal{CN}(0, N_0)$, in which $\mathcal{CN}(\mu, \sigma^2)$ represents a complex Gaussian random variable with a mean of μ and variance of σ^2.

We note that before transmitting data, training is performed for acquiring the CSI. This process requires pilot symbols [26] to be transmitted in a time-division duplexing (TDD) manner. However, in practice, the channel estimation suffers from CEEs [27], which is explicitly considered in our system model. The CEEs can be modeled by the superposition of numerous small quantities representing different noise sources and interference [28]-[30], Thus, based on the central limit theorem, it can be modeled by a Gaussian process [28]. Accordingly, the channels between $\mathcal{S}$, $\mathcal{R}$ and $\mathcal{R}$, $\mathcal{D}$ can be defined based on their imperfect estimates as $h_{SR} = \hat{h}_{SR} + e_{SR}$ and $h_{RD} = \hat{h}_{RD} + e_{RD}$ [28]-[30],where

$$e_i \sim \mathcal{CN}(0, \sigma^2_{e_i}), \qquad i \in \{SR, RD\}, \tag{1}$$

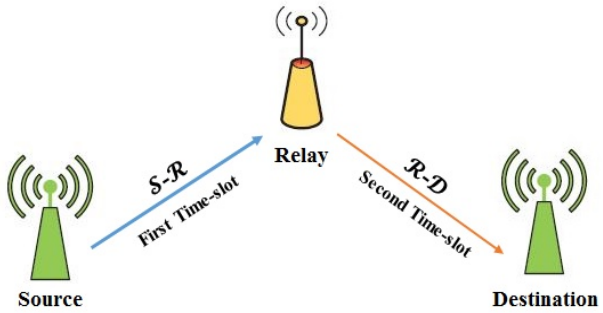

Fig. 1: System model consisting of Tx, Rx and AF relay nodes.

and σ_e^2 denotes the CEE variance.

To consider the impact of HWI on the received SNR, we model the residual HWI in $\mathcal{S}$, $\mathcal{R}$, $\mathcal{D}$ as presented in [31]. The transmitted distortion noise can be approximated by a Gaussian-distributed random variable. The experimental studies in [32] and analytical derivations in [32] and [33] confirm this. Accordingly, for modeling the transmitted imperfections we introduce the following parameter [32]

$$\eta_i^t \sim \mathcal{CN}(0, P_i k_i^{t2}), \qquad i \in \{\mathcal{S}, \mathcal{R}\}, \tag{2}$$

where P_i represents the transmit power of node i. The factor k_i^t determines the level of imperfections imposed by the transmitter hardware for $i \in \{\mathcal{S}, \mathcal{R}\}$. Furthermore, k_i^r represents the level of imperfections in the receiver hardware. These two parameters are equivalent to the error vector magnitude (EVM) characterizing the quality of RF transceivers[19].

We assume a time-division multiple-access (TDMA) protocol in our relaying scenario, during which $\mathcal{S}$ transmits the unit-power information signal x at the power P_S to $\mathcal{R}$. Accordingly, the signal received by $\mathcal{R}$ can be represented as

$$y_R = (\sqrt{P_S}x + \eta_S^t)h_{SR} + \eta_R^r + n_R, \tag{3}$$

where n_R represents the additive white Gaussian noise (AWGN) of $\mathcal{R}$ having a zero mean and variance of N_0. The term η_R^r models the imperfection at the receiver of $\mathcal{R}$, which obeys a complex Gaussian distribution, and thus can be represented as

$$\eta_R^r \sim \mathcal{CN}(0, {k_R^r}^2 P_S |h_{SR}|^2). \tag{4}$$

We note that the aggregated distortion represented by the hardware impairment terms in (3) for a given channel estimate $\hat{h}_{SR}$, has the power of

$$\mathbb{E}_{\eta_S^t,\eta_R^r}\left\{\left|\eta_S^t h_{SR} + \eta_R^r\right|^2\right\} = P_S(|\hat{h}_{SR}|^2 + \sigma_{e_{SR}}^2)({k_S^t}^2 + {k_R^r}^2). \tag{5}$$

In the second phase, $\mathcal{R}$ forwards the scaled version of the received signal to $\mathcal{D}$ with the amplification factor G given as

$$G = \sqrt{\frac{P_R}{P_S(|\hat{h}_{SR}|^2 + \sigma_{e_{SR}}^2)(1 + {k_S^t}^2 + {k_R^r}^2) + N_0}}, \tag{6}$$

where P_R is the transmit power of $\mathcal{R}$ in the second phase. Accordingly, the signal received by $\mathcal{D}$ can be written as

$$y_D = (y_R G + \eta_R^t)h_{RD} + \eta_D^r + n_D, \tag{7}$$

where, the term η_D^r models the receiver imperfections of $\mathcal{D}$, which has again a complex Gaussian distribution, and thus can be represented as

$$\eta_D^r \sim \mathcal{CN}(0, {k_D^r}^2 P_R |h_{RD}|^2). \tag{8}$$

Now, we can write the expression for SNDR for the signal received by $\mathcal{D}$ as

$$\gamma_{SD} = \frac{\alpha_1 |\hat{h}_{SR}|^2 |\hat{h}_{RD}|^2}{\alpha_2 |\hat{h}_{SR}|^2 |\hat{h}_{RD}|^2 + \alpha_3 |\hat{h}_{SR}|^2 + \alpha_4 |\hat{h}_{RD}|^2 + \alpha_0}. \tag{9}$$

In (9), if we define $\gamma_S = P_S/N_0$ and $\gamma_R = P_R/N_0$ as the transmit SNR at $\mathcal{S}$ and $\mathcal{R}$ respectively, then the values of α_1 through α_4 are given by (10)-(14).

In the first part of our study we will assume that the channel coefficients h_{SR} and h_{RD} are Nakagami-m random variables. Then, we will derive the asymptotic BLER expression for this case. To this end, we firstly have to extract the CDF of the SNDR in (9), when $|\hat{h}_{SR}|$ and $|\hat{h}_{RD}|$ are Nakagami-m variables and their squares ($X_1 = |\hat{h}_{SR}|^2, X_2 = |\hat{h}_{RD}|^2$) obey the Gamma distribution

$$f_{X_i}(x) = \frac{x^{m_i - 1} e^{-\frac{x}{\theta_i}}}{\Gamma(m_i)\theta_i^{m_i}}, \tag{15}$$

where, $\Gamma(.)$ denotes the Gamma function, m_i is the shape parameter assumed to be an integer number throughout our work and θ_i is the scale parameter. So, by considering the distribution of $|\hat{h}_i|^2$ as in (15), the CDF of the SNDR in (9) may be calculated as

$$P(\gamma < \gamma_{th}) = \begin{cases} 1 - g(\gamma_{th}), & \gamma_{\rm th} < \frac{\alpha_1}{\alpha_2} \\ 1, & \gamma_{\rm th} > \frac{\alpha_1}{\alpha_2} \end{cases}, \tag{16}$$

where, $g(\gamma_{th})$ is defined in (17) at the top of the next page.

Proof: See Appendix A.

It is worth mentioning that an expression can be found in [34] for the CDF of the SNDR in (9), when the channel coefficients obey the Nakagami-m distribution. However, as the CDF does not have a piecewise form as in (16), we derived the CDF in detail in Appendix A.

Following the derivation of asymptotic expression for the BLER in a Nakagami-m fading channel, we will proceed now by deriving the exact BLER of an AF relay in a Rayleigh fading channel for the cases of imperfect channel estimation at $\mathcal{R}$ and $\mathcal{D}$ as well as for having hardware impairments in $\mathcal{S}$, $\mathcal{R}$ and $\mathcal{D}$. Upon defining $\beta_1 = \sigma^2_{\hat{h}_{SR}}$ and $\beta_2 = \sigma^2_{\hat{h}_{RD}}$ as the mean of $|\hat{h}_{SR}|^2$ and $|\hat{h}_{RD}|^2$ respectively, then the CDF of the SNDR expression in (9) for a Rayleigh channel in case of $\gamma_{\rm th} < \frac{\alpha_1}{\alpha_2}$ can be expressed as [35]

$$P(\gamma < \gamma_{th}) = 1 - 2\frac{e^{-\frac{\beta_2\alpha_4 + \beta_1\alpha_3}{\beta_1\beta_2(\alpha_1 - \alpha_2\gamma_{th})}\gamma_{th}}}{\beta_1(\alpha_1 - \alpha_2\gamma_{th})}\sqrt{\frac{\gamma_{th}^2(\alpha_3\alpha_4 - \alpha_0\alpha_2) + \alpha_0\alpha_1\gamma_{th}}{\beta_2}\beta_1} \times K_1\Big(\frac{2}{\alpha_1 - \alpha_2\gamma_{th}}\sqrt{\frac{\gamma_{th}^2(\alpha_3\alpha_4 - \alpha_0\alpha_2) + \alpha_0\alpha_1\gamma_{th}}{\beta_1\beta_2}}\Big), \tag{18}$$

and for the case of $\gamma_{\rm th} > \frac{\alpha_1}{\alpha_2}$ it is equal to 1. In (18), $K_1(x)$ represents the first-order modified Bessel function of the second kind.

III. Nakagami-m Fading channel

In this section, we analyze the BLER performance of a realistic AF relay having hardware impairments and imperfect channel estimation under the finite block-length regime in a Nakagami-m fading channel for integer values of the shape parameter in both hops. Firstly, we will formulate the exact BLER expression and in the second subsection we will extract asymptotic BLER expressions to gain further insights.

A. Exact Analysis

Again, Polyanskiy *et al.* [5] determined the maximum channel coding rate achievable at a given finite blocklength and error probability. To elaborate a little further, when the packet length is high enough, each packet will experience a more or less similar wireless channel quality. Upon gradually increasing the packet length, this will lead to improved reception quality and eventually approaching the channel capacity, when the packet length asymptotically tends to infinity [36]. By contrast, when the packet length is short, these channel effects can not be averaged out and the average performance will be dominated by the low-quality received packets. Accordingly, the achievable rate will be reduced for short packets compared

$$\alpha_1 = \gamma_S\gamma_R \tag{10}$$

$$\alpha_2 = \gamma_S\gamma_R[(k_R^{t\,2} + k_D^{r\,2})(1 + k_S^{t\,2} + k_R^{r\,2}) + k_S^{t\,2} + k_R^{r\,2}], \tag{11}$$

$$\alpha_3 = \gamma_S\gamma_R\sigma^2_{e_{RD}}[(k_R^{t\,2} + k_D^{r\,2})(1 + k_S^{t\,2} + k_R^{r\,2}) + k_S^{t\,2} + k_R^{r\,2} + 1] + \gamma_S(k_S^{t\,2} + k_R^{r\,2} + 1), \tag{12}$$

$$\alpha_4 = \gamma_S\gamma_R\sigma^2_{e_{SR}}[(k_R^{t\,2} + k_D^{r\,2})(1 + k_S^{t\,2} + k_R^{r\,2}) + k_S^{t\,2} + k_R^{r\,2} + 1] + \gamma_R(k_R^{t\,2} + k_D^{r\,2} + 1), \tag{13}$$

$$\begin{aligned}\alpha_0 =& \gamma_S\gamma_R\sigma^2_{e_{SR}}\sigma^2_{e_{RD}}[(k_R^{t\,2} + k_D^{r\,2})(1 + k_S^{t\,2} + k_R^{r\,2}) + k_S^{t\,2} + k_R^{r\,2} + 1] + \gamma_R\sigma^2_{e_{RD}}(1 + k_R^{t\,2} + k_D^{r\,2}) \\ &+ \gamma_s\sigma^2_{e_{SR}}(1 + k_S^{t\,2} + k_R^{r\,2}) + 1,\end{aligned} \tag{14}$$

$$\begin{aligned}g(\gamma_{th}) = 2\frac{(\alpha_4\gamma_{th})^{m_1-1}(\alpha_3\gamma_{th})^{m_2-1}}{(\alpha_1-\alpha_2\gamma_{th})^{m_1+m_2-1}}\frac{e^{-\frac{\theta_2\alpha_4+\theta_1\alpha_3}{\theta_1\theta_2(\alpha_1-\alpha_2\gamma_{th})}\gamma_{th}}}{\Gamma(m_1)\Gamma(m_2)\theta_1^{m_1}\theta_2^{m_2-1}}\sum_{k=0}^{m_2-1}\sum_{i=0}^{m_1-1}\sum_{j=0}^{m_2-k-1}k!\binom{m_2-1}{k} \\ \times\binom{m_1-1}{i}\binom{m_2-k-1}{j}\frac{(\alpha_1-\alpha_2\gamma_{th})^k\left[\gamma_{th}^2(\alpha_3\alpha_4-\alpha_0\alpha_2)+\alpha_0\alpha_1\gamma_{th}\right]^{\frac{i+j+1}{2}}}{(\alpha_4\gamma_{th})^i(\alpha_3\gamma_{th})^{j+k}}\theta_2^k\left(\frac{\theta_1}{\theta_2}\right)^{\frac{i-j+1}{2}} \\ \times K_{i-j+1}\left(\frac{2}{\alpha_1-\alpha_2\gamma_{th}}\sqrt{\frac{\gamma_{th}^2(\alpha_3\alpha_4-\alpha_0\alpha_2)+\alpha_0\alpha_1\gamma_{th}}{\theta_1\theta_2}}\right)\end{aligned} \tag{17}$$

to Shannon capacity [1]. This new bound on the achievable rate in SPC is formulated in [5] as

$$r = C(\gamma) - Q^{-1}(\epsilon)\sqrt{v(\gamma)/m}. \tag{19}$$

We reformulate (19) in order to obtain the BLER in terms of the channel coding rate and the block-length as [7, eq. 15]

$$\epsilon = Q\left(\frac{C(\gamma)-r}{\sqrt{v(\gamma)/m}}\right), \tag{20}$$

where, $Q(.)$ denotes the Gaussian Q-function, $C(\gamma) = \log_2(1+\gamma)$ is the Shannon capacity and $v(\gamma) = (\log_2 e)^2[1 - 1/(1+\gamma)^2]$ is the channel-induced dispersion. It is assumed that the source and destination exchange N bits of information over $\hat{m}$ channel uses in each packet transmission. This leads to $m = \frac{\hat{m}}{2}$, where m is the duration of each time slot, quantified in terms of the channel uses. Furthermore, $r = \frac{N}{m}$ denotes the coding rate. It is worth noting that when the packet length is asymptotically high ($m \to \infty$), the SPC maximum rate in (19) will tend to the Shannonian capacity and the BLER in (20) will become zero, which is a plausible observation based on our previous discussions.,

In the following, we average the instantaneous BLER of (20) in order to characterize the average BLER. Since (20) can not be evaluated in a closed form, we opt for the linear approximation of (20) given by [37]

$$\epsilon \approx \chi(\gamma) = \begin{cases} 1 & \gamma \le \psi \\ \frac{1}{2} - \frac{\alpha_m}{\sqrt{2\pi}}(\gamma - \theta_m) & \psi < \gamma < \omega \\ 0 & \omega \le \gamma \end{cases}, \tag{21}$$

where, $\theta_m = 2^r - 1$, $\alpha_m = \frac{\sqrt{m}}{\sqrt{2^{2r}-1}}$, $\psi = \theta_m - \frac{1}{\alpha_m}\sqrt{\frac{\pi}{2}}$, and $\omega = \theta_m + \frac{1}{\alpha_m}\sqrt{\frac{\pi}{2}}$. In (21), we face with the approximation of the BLER in (20) utilizing the first-order Taylor series expansion around θ_m. Accordingly, we expect that as the SNDR level deviates from $\gamma = \theta_m$, the approximation error will be aggravated. This error should be dealt with carefully, especially when the SNDR is close to ω or ψ, where the BLER function makes a sharp turn. We will examine the tightness of this approximation in more details in Section V and Subsection C. Additionally, we will discuss those special cases in our scenario, when using (21) will lead to inaccurate results. Now, with the aid of the above-mentioned approximation, the average BLER can be expressed as

$$\begin{aligned}\mathbb{E}\left\{Q\left(\frac{C(\gamma)-r}{\sqrt{v(\gamma)/m}}\right)\right\} &= \int_0^\infty Q\left(\frac{C(x)-r}{\sqrt{v(x)/m}}\right)f_\gamma(x)dx \\ &\approx \int_0^\infty \chi(x)f_\gamma(x)dx.\end{aligned} \tag{22}$$

As the direct solution of the above integral is mathematically tedious, we exploit the partial integration theorem and reformulate (22) as

$$\begin{aligned}\epsilon_{ave} &\approx \int_0^\infty \chi(x)f_\gamma(x)dx = \Big[\chi(x)F_\gamma(x)\Big]_0^\infty \\ &- \int_0^\infty F_\gamma(x)d\chi(x) \\ &= \frac{\alpha_m}{\sqrt{2\pi}}\int_\psi^\omega F_\gamma(x)dx\end{aligned} \tag{23}$$

Considering the expression given in (16) and (17), the exact BLER for a Nakagami-m fading channel can be calculated by numerically analyzing the integral in (23). Since deriving an exact BLER expression by analytically solving the integral in (23) is still tedious, in the next subsection we will focus our attention on the high-SNR analysis of our problem to extract an asymptotic BLER expression for a Nakagami-m fading channel.

B. High-m Case Analysis

In this part, we seek to derive the analytical average BLER through the integral in (23). If the block-length m is sufficiently high in the approximate BLER expression of (21) (a condition that is generally fulfilled as (19) and (20) are tight for $m > 100$ [5], [7]), then the integration interval in (23) will become small. Thus the first-order Riemann integral approximation can be employed, [38].

$$\int_{\psi}^{\omega} F_{\gamma}(x)dx \approx (\omega - \psi)F_{\gamma}(\frac{\psi+\omega}{2}). \tag{24}$$

We note that for the integration interval of $(\omega - \psi = \sqrt{2\pi(2^{2N/m}-1)}/\sqrt{m})$ to become small, in addition to m being large, N should be a small number, which is equal to r or alternatively the data rate has to be low. By applying the first order Riemann approximation of (24), we can write the average BLER as in (25) at the top of the next page, where we have $\theta_m = \frac{\psi+\omega}{2}$.

We note that for a sufficiently large m, the upper limit of the integral will also become quite small. Hence, in (16) the specific part of the CDF associated with $\gamma_{\mathrm{th}} < \frac{\alpha_1}{\alpha_2}$ applies in the low-data-rate case. We will discuss the tightness of (24) in more details in Section VII.

C. High Data Rate Case Analysis

In the specific case of a high data rate, the lower limit of the integral in (23) will become large. If ψ gets larger than the ratio $\frac{\alpha_1}{\alpha_2}$ in (16), for the integral in (23) we have

$$\epsilon_{ave} \approx \frac{\alpha_m}{\sqrt{2\pi}} \int_{\psi}^{\omega} F_{\gamma}(x)dx = \frac{\alpha_m}{\sqrt{2\pi}}(\omega - \psi) = 1. \tag{26}$$

This is an important result when dealing with a system having realistic imperfect hardware components. The average BLER expression in (26) suggests that for high data rates in a short-packet cooperative AF scenario having HWIs, if the transmission rate is so high or equivalently the hardware impairment factor is significant so that $\psi > \frac{\alpha_1}{\alpha_2}$, the system will fail to operate adequately, regardless of the transmit power of the source and relay nodes (note that ψ grows exponentially by the increase in transmission rate. Furthermore, by the increase in HWI, $\frac{\alpha_1}{\alpha_2}$ will decrease according to (10) and (11)). This observation enforces an upper bound on the maximum achievable rate and should not be confused with the maximum achievable rate inherent in SPC, which is implied through (19). In fact, as stated earlier, this upper bound is imposed on our scenario due to the HWIs present in all nodes and it is independent of the transmit power - unlike the bound in (19).

IV. Rayleigh Fading channel

To extract the expressions of BLER for a specific fading distribution, we have to solve the integral in (23) for determining its associated CDF. In the previous section we saw that the analytical solution of this integral when our channel coefficients in (9) follow Nakagami-m distribution is tedious. This also holds for the Rayleigh distribution. This motivated us to analyze our scenario of joint hardware impairment and channel estimation error for a Rayleigh channel in a pair of specific scenarios, namely for the "BLER in the presence of hardware impairments" and the "BLER with channel estimation errors" scenarios.

A. Hardware Impairment with Perfect Channel Estimation

Here we assume that the channel estimation is perfect, which means that the expression for α_0 in (14) is equal to zero. So $F_{\gamma}(x)$ in (18) can be rewritten as

$$F_{\gamma_A}(x) = \begin{cases} 1 - 2\frac{e^{-\frac{\beta_2\alpha_4+\beta_1\alpha_3}{\beta_1\beta_2(\alpha_1-\alpha_2 x)}x}}{\beta_1(\alpha_1-\alpha_2 x)} x\sqrt{\frac{\alpha_3\alpha_4\beta_1}{\beta_2}} K_1\big(\frac{2x}{\alpha_1-\alpha_2 x}\sqrt{\frac{\alpha_3\alpha_4}{\beta_1\beta_2}}\big), & \gamma_{\mathrm{th}} \\ 1, & \gamma_{\mathrm{th}} \end{cases} \tag{27}$$

By changing variables $u(x) = \frac{2x}{\alpha_1-\alpha_2 x}\sqrt{\frac{\alpha_3\alpha_4}{\beta_1\beta_2}}$ in the integral of (23) we arrive at :

$$\int_{\psi}^{\omega} F_{\gamma_A}(x)dx = \eta_3\eta_2^2 \int_{u(\psi)}^{u(\omega)} \Big[1 - ue^{-\eta_1 u}K_1(u)\Big]\frac{du}{(u+\eta_2)^2}, \tag{28}$$

where, $\eta_1 = \frac{\beta_2\alpha_4+\beta_1\alpha_3}{2}\sqrt{\frac{1}{\beta_1\beta_2\alpha_3\alpha_4}}$, $\eta_2 = \frac{2}{\alpha_2}\sqrt{\frac{\alpha_3\alpha_4}{\beta_1\beta_2}}$ and $\eta_3 = \frac{\alpha_1}{2}\sqrt{\frac{\beta_1\beta_2}{\alpha_3\alpha_4}}$. To find a closed-form expression of the integral in (28), we use a series representation of $\frac{ue^{-\eta_1 u}}{(u+\eta_2)^2}$ as

$$\frac{ue^{-\eta_1 u}}{(u+\eta_2)^2} = \sum_{i=1}^{\infty}\sum_{j=1}^{i} \frac{j(-1)^{i+1}\eta_1^i}{\eta_2(\eta_1\eta_2)^j(i-j)!}u^i. \tag{29}$$

Now, the integral in (28) can be evaluated from (29) as

$$\epsilon_{ave} \approx 1 - \frac{\alpha_m}{\sqrt{2\pi}}\eta_3\eta_2^2 \sum_{i=1}^{\infty}\sum_{j=1}^{i} \frac{j(-1)^{i+1}\eta_1^i}{\eta_2(\eta_1\eta_2)^j(i-j)!} \times \int_{w(\psi)}^{w(\omega)} u^i K_1(u)du. \tag{30}$$

where $w(x) = \eta_2\frac{x}{\frac{\alpha_1}{\alpha_2}-x}$.To solve the integral in (30), instead of writing $u^i K_1(u)$ in terms of the Meijer-G function as in [12] and dealing with tedious mathematical operations to solve the integral, we can use the results in [39]. For $\nu > 0$ and $\nu \notin \left\{0, \frac{1}{2}, \frac{3}{2}\right\}$, we have

$$K_{\nu}(\beta x) = \exp(-\beta x)\sum_{n=0}^{\infty}\sum_{m=0}^{n} \Lambda(\nu, n, m)(\beta x)^{m-\nu}, \tag{31}$$

where $\Lambda(\nu, n, m) = \frac{(-1)^m\sqrt{\pi}\Gamma(2\nu)\Gamma(n-\nu+\frac{1}{2})\mathrm{L}(n,m)}{2^{\nu-m}\Gamma(\frac{1}{2}-\nu)\Gamma(n+\nu+\frac{1}{2})n!}$ in which $\mathrm{L}(n,m) = \binom{n-1}{m-1}\frac{n!}{m!}$ for $n, m > 0$ represents the Lah numbers [40]. The final expression is presented in (32) at the top of page 7. We note that the result in (32) is valid for $\omega \leq \frac{\alpha_1}{\alpha_2}$. To obtain the average BLER for the case of $\omega > \frac{\alpha_1}{\alpha_2}$, firstly (32) should be evaluated by setting $\omega = \frac{\alpha_1}{\alpha_2}$ and then added to $\frac{\alpha_m}{\sqrt{2\pi}}(\omega - \frac{\alpha_1}{\alpha_2})$. The term $\frac{\alpha_m}{\sqrt{2\pi}}(\omega - \frac{\alpha_1}{\alpha_2})$ is the resultant expression after substituting the part of (27) with $\gamma_{th} > \frac{\alpha_1}{\alpha_2}$ into (23). This term is independent of the transmit power of both the $\mathcal{S}$ and $\mathcal{R}$ nodes and shows that if the system is designed so that $\omega > \frac{\alpha_1}{\alpha_2}$, a serious error floor will occur at the $\mathcal{D}$ node.

It is worth mentioning that no closed-form expressions were

$$\epsilon_{ave} \approx 1 - 2\frac{(\alpha_4\theta_m)^{m_1-1}(\alpha_3\theta_m)^{m_2-1}}{(\alpha_1-\alpha_2\theta_m)^{m_1+m_2-1}} \frac{e^{-\frac{\theta_2\alpha_4+\theta_1\alpha_3}{\theta_1\theta_2(\alpha_1-\alpha_2\theta_m)}\theta_m}}{\Gamma(m_1)\Gamma(m_2)\theta_1^{m_1}\theta_2^{m_2-1}} \sum_{k=0}^{m_2-1}\sum_{i=0}^{m_1-1}\sum_{j=0}^{m_2-k-1} k!\binom{m_2-1}{k} \times \binom{m_1-1}{i}\binom{m_2-k-1}{j} \frac{(\alpha_1-\alpha_2\theta_m)^k\left[\theta_m^2(\alpha_3\alpha_4-\alpha_0\alpha_2)+\alpha_0\alpha_1\theta_m\right]^{\frac{i+j+1}{2}}}{(\alpha_4\theta_m)^i(\alpha_3\theta_m)^{j+k}}\theta_2^k\left(\frac{\theta_1}{\theta_2}\right)^{\frac{i-j+1}{2}} \times K_{i-j+1}\left(\frac{2}{\alpha_1-\alpha_2\theta_m}\sqrt{\frac{\theta_m^2(\alpha_3\alpha_4-\alpha_0\alpha_2)+\alpha_0\alpha_1\theta_m}{\theta_1\theta_2}}\right), \tag{25}$$

$$\epsilon_{ave} \approx 1 - \frac{\alpha_m}{\sqrt{2\pi}}\eta_3\eta_2^2\sum_{i=1}^{\infty}\sum_{j=1}^{i}\frac{j(-1)^{i+1}\eta_1^i}{\eta_2(\eta_1\eta_2)^j(i-j)!}\sum_{n=0}^{\infty}\sum_{m=0}^{n}\sum_{p=0}^{i+m-1}\Lambda(1,n,m)p!\binom{i+m-1}{p} \times\left[e^{-w(\psi)}\big(w(\psi)\big)^{i+m-p-1}-e^{-w(\omega)}\big(w(\omega)\big)^{i+m-p-1}\right] \tag{32}$$

derived for BLER performance in the presence of hardware impairments in the related literature.

B. Imperfect Channel Estimation with Perfect Hardware

Another problem which may be frequently encountered in practical scenarios is the presence of imperfect channel estimation. To address this case, we have to rewrite the expression of $F_\gamma(x)$ in (18) by setting $\alpha_2 = 0$ in (11), yielding

$$F_{\gamma_B}(x) = 1 - 2\frac{e^{-\frac{\beta_2\alpha_4+\beta_1\alpha_3}{\beta_1\beta_2\alpha_1}x}}{\beta_1\alpha_1}\sqrt{\frac{\alpha_3\alpha_4x^2+\alpha_0\alpha_1x}{\beta_2}\beta_1} .K_1\left(\frac{2}{\alpha_1}\sqrt{\frac{\alpha_3\alpha_4x^2+\alpha_0\alpha_1x}{\beta_1\beta_2}}\right). \tag{33}$$

Now, we have to insert the expression of $F_{\gamma_B}(x)$ in (33) into the integral of (23) to find the average BLER. After applying the steps presented in Appendix B, ϵ_{ave} of (23) can be written as

$$\epsilon_{ave} \approx 1 - \frac{\alpha_m}{\sqrt{2\pi}}\frac{\alpha_1\beta_1\beta_2}{2}\sum_{k=0}^{\infty}\sum_{i=0}^{k}\sum_{j=0}^{\infty}\frac{(-1)^k}{k!}\left(\frac{\beta_2\alpha_4+\beta_1\alpha_3}{2\alpha_1\alpha_3\alpha_4\beta_1\beta_2}\right)^k \binom{k}{i}\alpha_1^i(-\alpha_0\alpha_1)^{k-i}\frac{\Gamma(q+1)}{\Gamma(q-j+1)j!}(\alpha_0^2)^j(\alpha_3\alpha_4\beta_1\beta_2)^{q-j} \times\int_{h(\psi)}^{h(\omega)}h^{2(q-j+1)}K_1(h)dh, \tag{34}$$

where $q = \frac{i-1}{2}$ and $h(x)$ is defined in Appendix B. We note that to solve the integral in (34), we can use again the equivalent expression for the modified Bessel function of the second kind in (31). The final expression is represented in (35) at the top of the next page.

Again, we note that no closed-form BLER expressions were derived in the related literature in the presence of hardware impairments.

V. Asymptotic Analysis

To obtain some insights concerning the fundamental impact of CEEs and HWIs on our cooperative system model, we now elaborate on the high-SNR regime in this section. Explicitly, we will drive an asymptotic expression for the BLER in a Rayleigh channel and will determine the optimum system parameters for minimizing the BLER.

A. High SNR Regime

The complexity of the expression representing the CDF of SNDR in a Rayleigh channel (18) makes the derivation of an analytical BLER expression quite a challenge, when both CEEs and HWIs are present. This motivated us to analyze the BLER performance in the high-SNR regime and glean useful insights into the system performance by the asymptotic analysis of the BLER. The high-SNR expression of the CDF in (18) (i.e. $P_S, P_R \gg 1$) for low CEE (i.e. $\sigma^2_{e_{SR}}, \sigma^2_{e_{RD}} \ll 1$) can be written as

$$F_{\gamma_{SD_\infty}}(x) = \frac{\beta_2\alpha_4+\beta_1\alpha_3}{\beta_1\beta_2(\alpha_1-\alpha_2x)}x = \frac{\beta_1\sigma^2_{e_{RD}}+\beta_2\sigma^2_{e_{SR}}}{\beta_1\beta_2(1-xd)}d_1d_2x + \frac{\beta_1d_1\gamma_S+\beta_2d_2\gamma_R}{\beta_1\beta_2(1-xd)\gamma_S\gamma_R}x, \tag{36}$$

where, $d_1 = {k_S^t}^2 + {k_R^r}^2 + 1$, $d_2 = {k_R^t}^2 + {k_D^r}^2 + 1$ and $d = d_1d_2 - 1$. Now, substituting the high-SNR CDF expression of (36) into (23), will lead to the asymptotic BLER expression for our scenario

$$\epsilon_{ave_\infty} = \frac{\beta_2\alpha_4+\beta_1\alpha_3}{\beta_1\beta_2\alpha_2^2}\Big(\frac{\alpha_1\alpha_m}{\sqrt{2\pi}}\ln\frac{\alpha_1-\alpha_2\psi}{\alpha_1-\alpha_2\omega}-\alpha_2\Big), \tag{37}$$

or to

$$\epsilon_{ave_\infty} = \Big(\frac{d_1}{\beta_2\gamma_Rd^2}+\frac{d_2}{\beta_1\gamma_Sd^2}\Big)\Big(\frac{\alpha_m}{\sqrt{2\pi}}\ln\frac{1-d\psi}{1-d\omega}-d\Big) \underbrace{+\frac{d+1}{d^2}\Big(\frac{\sigma^2_{e_{SR}}}{\beta 1}+\frac{\sigma^2_{e_{RD}}}{\beta 2}\Big)\Big(\frac{\alpha_m}{\sqrt{2\pi}}\ln\frac{1-d\psi}{1-d\omega}-d\Big)}_{\text{error floor term}} \tag{38}$$

$$\epsilon_{ave} \approx 1 - \frac{\alpha_m}{\sqrt{2\pi}} \frac{\alpha_1\beta_1\beta_2}{2} \sum_{k=0}^{\infty}\sum_{i=0}^{k}\sum_{j=0}^{\infty} \frac{(-1)^k}{k!} \left(\frac{\beta_2\alpha_4+\beta_1\alpha_3}{2\alpha_1\alpha_3\alpha_4\beta_1\beta_2}\right)^k \binom{k}{i} \alpha_1^i(-\alpha_0\alpha_1)^{k-i} \times \frac{\Gamma(q+1)}{\Gamma(q-j+1)j!}(\alpha_0^2)^j(\alpha_3\alpha_4\beta_1\beta_2)^{q-j} \sum_{n=0}^{\infty}\sum_{m=0}^{n}\sum_{p=0}^{i+m-2j} \Lambda(1,n,m)p!\binom{i+m-2j}{p} \times \left[e^{-h(\psi)}\big(h(\psi)\big)^{i+m-p-2j} - e^{-h(\omega)}\big(h(\omega)\big)^{i+m-p-2j}\right] \tag{35}$$

Here, we state a pair of important remarks concerning the condition of low CEE variance ($\sigma^2_{e_{SR}}, \sigma^2_{e_{RD}} \ll 1$) in obtaining (38):

Remark 1: Assuming low CEE variance in a cooperative scenario is a common assumption in the related literature [41]. Furthermore, in a practical scenario low CEE can be attained when the power level of the training phase is asymptotically high. The expression of the CEE variance in the $\mathcal{S}$-$\mathcal{R}$ and $\mathcal{R}$-$\mathcal{D}$ links can be expressed by considering the HWI effects as [41]

$$\sigma^2_{e_{SR}} = \frac{1+({k_S^t}^2+{k_R^r}^2)\gamma_P\Omega_1}{1+\big[n_t+({k_S^t}^2+{k_R^r}^2)\big]\gamma_P\Omega_1}, \tag{39}$$

$$\sigma^2_{e_{RD}} = \frac{1+({k_R^t}^2+{k_D^r}^2)\gamma_P\Omega_2}{1+\big[n_t+({k_R^t}^2+{k_D^r}^2)\big]\gamma_P\Omega_2}, \tag{40}$$

where, n_t is the training length and $\gamma_P = \frac{P_P}{N_0}$, in which P_P is the power of the training phase, while Ω_1 and Ω_2 are the mean of $|h_{SR}|^2$ and $|h_{RD}|^2$, respectively. When the transmit SNR is very high, the CEE variances in (39) and (40) reduce to [41]

$$\sigma^2_{e_{SR}} \simeq \frac{{k_S^t}^2+{k_R^r}^2}{n_t+({k_S^t}^2+{k_R^r}^2)} \approx \frac{{k_S^t}^2+{k_R^r}^2}{n_t}, \tag{41}$$

$$\sigma^2_{e_{RD}} \simeq \frac{{k_R^t}^2+{k_D^r}^2}{n_t+({k_R^t}^2+{k_D^r}^2)} \approx \frac{{k_R^t}^2+{k_D^r}^2}{n_t}. \tag{42}$$

We note that, without the assumption of $\sigma^2_{e_{SR}}$ and $\sigma^2_{e_{RD}}$ being very small, the BLER floor term in (38) will have a significant value. Furthermore (38) shows that, this error floor becomes more severe in the presence of considerable HWI in the nodes. To mitigate this effect in the high-SNR regime, one should consider minimizing the CEE and HWI. According to (39) and (40) the CEE variance itself becomes more serious upon increasing the HWI level in the nodes. Observe that according to (41) and (42) increasing the training power, reduces the CEE variances, but they still remain non-negligible, if the HWI is significant. We note that for reasonably long training sequences applied in an SPC scenario, e.g., $n_t > 10$ [22] and assuming typical impairment levels, the CEE variance terms can be considered to be very low, which was indeed was exploited in deriving our asymptotic expression. We also emphasize that reducing the impairment level is also capable of mitigating both the CEE variances and the BLER floor in (38).

Remark 2: As we stated in Remark 1, typical values found in the literature for n_t result in low CEE variances at high training power, even in the presence of HWI. But one may assume that the delay in the transmission process, which is an important factor in a short-packet application, will become low upon reducing the n_t value and this can challenge the aforementioned assumption. Here, we note that according to (39) and (40), reducing the training length will lead to higher CEE variances. In a practical layered scheme presented in [22], one has to account for the consequences of transmission errors and low data rates as regards to the transmit bufferqueue-length, since the data is only removed from the buffer once an acknowledgment indicates its correct reception. Due to the increased CEE variances imposed by reducing the training length, the probability of error at the receiver becomes higher, hence leading to repeated transmission of the same data block and therefore increasing the delay rather than decreasing it.

B. High SNR and High-m regime

In the previous section, we formulated the high-SNR BLER in a Rayleigh fading channel. However, to obtain further insights concerning the impact of CEE and HWI, we have to evaluate the BLER in the high-SNR regime, when the block-length "m" is sufficiently high. The assumption of "m" being sufficiently large in subsection "A" has a good accuracy comparing with the exact analytical result as being showed in the following sections and is used in the related work [38].

By considering the high-SNR regime (i.e. $P_S, P_R \gg 1$) as well as low CEE (i.e. $\sigma^2_{e_{SR}}, \sigma^2_{e_{RD}} \ll 1$) and assuming a sufficiently high "m", the asymptotic average BLER for a Rayleigh channel can be written as

$$\epsilon_{ave_\infty} = \frac{\beta_2\alpha_4+\beta_1\alpha_3}{\beta_1\beta_2(\alpha_1-\alpha_2\theta_m)}\theta_m = \frac{d_1\theta_m}{\beta_2\gamma_R(1-\theta_m d)} + \frac{d_2\theta_m}{\beta_1\gamma_S(1-\theta_m d)} + \underbrace{\frac{\beta_1\sigma^2_{e_{RD}}+\beta_2\sigma^2_{e_{SR}}}{\beta_1\beta_2(1-\theta_m d)}d_1d_2\theta_m}_{\text{error floor term}}. \tag{43}$$

The expression in (43) gives us useful insights concerning the system performance in the high-SNR regime, since it is more simple than (38), even though the difference between the two performance metrics is negligible, as it will be shown in Section VII.

Expressions (38) and (43) show that there is a BLER floor, which depends both on the CEE and on the level of HWI. We note that even though the HWI alone does not produce a BLER floor, but it aggravates the CEE effects. Thus having a considerable level of HWI will mask the benefits of

having a low level of CEE, if the HWI and CEE are studied independently.

C. Asymptotic SNR Regime

1) Perfect Hardware: In this subsection, we want to gain practical insights into the effects of CSI errors on the BLER by analyzing our scenario for asymptotic SNRs. Here we assume that HWI is equal to zero and study the special case of our discussion in Section 4-A for a Rayleigh channel.

Corollary 1. *Let us assume that γ_S, γ_R grow large with $\gamma_S = \beta\gamma_R$ for some $\beta > 0$, while the relay gain in* (6) *remains finite and strictly positive. The instantaneous SNDR can be written as*

$$\lim_{\substack{\gamma_S,\gamma_R\to\infty \\ k_1^2=k_2^2=0}} \gamma_{SD} = \frac{|\hat{h}_{SR}|^2|\hat{h}_{RD}|^2}{\sigma^2_{e_{RD}}|\hat{h}_{SR}|^2 + \sigma^2_{e_{SR}}|\hat{h}_{RD}|^2 + \sigma^2_{e_{SR}}\sigma^2_{e_{RD}}}. \tag{44}$$

To calculate the average BLER in this case, we can set $\alpha_1 = 1$, $\alpha_3 = \sigma^2_{e_{RD}}$, $\alpha_4 = \sigma^2_{e_{SR}}$ and $\alpha_0 = \alpha_3\alpha_4$ in (34). The resultant error floor expression caused by the imperfect CSI can be used for arbitrary values of $\sigma^2_{e_{SR}}$ and $\sigma^2_{e_{RD}}$. However, the expressions for the error floor terms in (38) and (43), require the assumption of having low CEE (i.e. $\sigma^2_{e_{SR}}, \sigma^2_{e_{RD}} \ll 1$) in both hops.

2) Perfect Channel State Information: In this subsection, we quantify the HWI effects on the BLER by analyzing our scenario for asymptotic SNRs. Here we assume that the CEE is equal to zero and study the special case of our discussion outlined in Section 4-B for a Rayleigh channel.

Corollary 2. *Let us assume that γ_S, γ_R grow large with $\gamma_S = \beta\gamma_R$ for some $\beta > 0$, while the relay gain in* (6) *remains finite and strictly positive. For any arbitrary random distribution of the estimated channel gains $\hat{h}_{SR}$, $\hat{h}_{RD}$, one can write the average BLER as*

$$\epsilon_{asy} = Q\left(\frac{\log_2(1+\gamma_{asy}) - r}{\sqrt{(\log_2 e)^2(1-1/(1+\gamma_{asy})^2)/m}}\right), \tag{45}$$

where, $\gamma_{asy} = \frac{1}{d}$.

Proof. Considering the SNDR value in (9) *and by setting $\sigma^2_{e_{SR}} = \sigma^2_{e_{RD}} = 0$ in* (10) *through* (14)*, followed by taking the limit $\gamma_S, \gamma_R \to \infty$ (assuming $\gamma_S = \beta\gamma_R$) will lead to instantaneous SNDR, which converges to*

$$\lim_{\substack{\gamma_S,\gamma_R\to\infty \\ \sigma^2_{e_{SR}}=\sigma^2_{e_{RD}}=0}} \gamma_{SD} = \frac{1}{d}. \tag{46}$$

Note that as the resultant SNDR is deterministic, the average BLER can be readily obtained through (20)*.*

Note that (46) exhibits a saturation effect for SNDRs in the asymptotic regime, which may limit the BLER parameter in (45). This phenomenon shows a fundamental difference between the non-ideal and ideal hardware scenarios, since for the latter the SNDR grows without bound upon increasing the transmit power of the $\mathcal{S}$ and $\mathcal{R}$ nodes. We also note that the SNDR ceiling in (46) and the resultant average BLER in (45), are independent of the channel coefficient distributions. So these results apply for both the Rayleigh and Nakagami-m distributions.

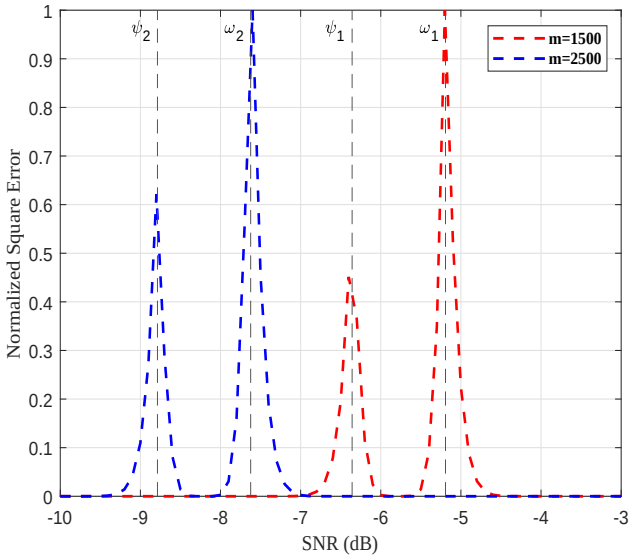

Fig. 2: Normalized square error between exact and approximate BLER expressions.

Remark 3: In Section II, Equation (21) was introduced, as it was intractable to evaluate the closed-form expression in (20). This linear approximation is widely used in the literature, but one should note the special cases, in which the error between the exact and approximate expressions is non-negligible. In (21), when $\psi < \gamma < \omega$, the closed-form expression is approximated by the first two terms of a Taylor series expansion around $\gamma_0 = \theta_m$. So we expect that by increasing the distance from $\gamma_0 = \theta_m$ the error will escalate.

Fig.2 shows the normalized square error between (20) and (21) for different values of the SNR for the two cases of channel use parameter m ($m = 1500$ and $m = 2500$). It is evident that when the SNR is close to ψ or ω, the error is maximized. So upon averaging the BLER through using the approximate expression, one should ensure that the mean of the SNDR in (9) is not close to ψ and ω.

In our scenario, this effect can make our analysis inaccurate when using Equation (30) to evaluate the exact average BLER for perfect CSI at high SNRs and at specific levels of the HWI. This is because according to (46), the mean of the SNDR at asymptotic power values becomes equal to $\frac{1}{d}$ and if this value is close to ω ($\omega \approx \frac{1}{d}$), then using (30) will lead to error in calculating the average BLER. Hence, when $\omega \approx \frac{1}{d}$ and the analysis considers low or medium values of SNDR, then Equation (30) is indeed accurate, but when dealing with high values of SNDR, we recommend using (45) instead.

VI. Optimum System Parameters

Optimal resource allocation in a resource-limited wireless network such as battery-limited IoTs and WSNs, is a salient network design aspect [42]. The network life-time clearly

depends on the power consumed by the nodes [43]. This motivated us to conceive and solve an optimization problem under a total transmit power constraint. Hence, we formulate an optimization problem for minimizing the average BLER in our scenario.

A. High-SNR and High-m Regime

In this subsection, we seek the optimal power and impairment sharing directly minimizing the average BLER. In the previous section we analyzed the average BLER in the "High-SNR Regime" as well as in the "High-SNR and High-m Regime". For the sake of providing practical insight concerning the optimum system parameters, we have considered the latter case in our study of the optimal system parameter allocation. To this end, we rewrite the average BLER expression in (43) in terms of f and g as

$$\epsilon_{ave_\infty} = f(\gamma_S, \gamma_R) + g(d_1, d_2), \tag{47}$$

where f is a monotonically decreasing function both with respect to γ_S as well as γ_R and g is independent of both γ_S as well as γ_R, representing the BLER floor term, which depends on the HWI parameters. We intend to minimize f under the total transmit power constraint of $\gamma_S + \gamma_R = \gamma_{tot}$. Furthermore, for minimizing g we assume having a fixed total EVM constraint of k_R at $\mathcal{R}$ besides having a joint EVM constraint k_{SR} in $\mathcal{S}$ and $\mathcal{D}$, so that $k_R^t + k_R^r = k_R$ and $k_S^t + k_D^r = k_{SD}$. To this end, we break the minimization problem of the expression in (47), into two separate steps and provide the associated solutions in the following corollaries.

Corollary 3. *Assume that $\gamma_S + \gamma_R = \gamma_{tot}$. Then $f(\gamma_S, \gamma_R)$ is minimized if $\gamma_S = \frac{\gamma_{tot}}{1+\sqrt{\frac{d_1\beta_1}{d_2\beta_2}}}$ and $\gamma_R = \frac{\gamma_{tot}}{1+\sqrt{\frac{d_2\beta_2}{d_1\beta_1}}}$.*

Proof. substituting $\gamma_S = \gamma_{tot} - \gamma_R$ into $f(\gamma_S, \gamma_R)$ and then taking the derivative of the resultant expression with respect to γ_S and setting it to zero will yield

$$(d_1\beta_1 - d_2\beta_2)\gamma_S^2 + 2d_2\beta_2\gamma_{tot}\gamma_S - d_2\beta_2\gamma_{tot}^2 = 0. \tag{48}$$

The quadratic equation in (48) will reduce to a first order equation if $d_1\beta_1 = d_2\beta_2$, leading to $\gamma_S = \gamma_R = \frac{\gamma_{tot}}{2}$. When $d_1\beta_1 \neq d_2\beta_2$, there exists two roots for the equation. To determine the feasible root, the equation can be solved both for $d_1\beta_1 > d_2\beta_2$ and $d_1\beta_1 < d_2\beta_2$. Then by taking the sign of $\frac{\partial f}{\partial \gamma_S}$ into account, one can readily see that $\gamma_S = \frac{\gamma_{tot}}{1+\sqrt{\frac{d_1\beta_1}{d_2\beta_2}}}$ and $\gamma_R = \frac{\gamma_{tot}}{1+\sqrt{\frac{d_2\beta_2}{d_1\beta_1}}}$ are the feasible solutions. We also note that the power allocation factors obtained satisfy the total power constraint ($\gamma_S + \gamma_R = \gamma_{tot}$) as their sum is equal to one and both factors are larger than zero but less than one for any arbitrary value of d_1, d_2, β_1 and β_2 (All of these parameters are strictly positive).

Corollary 4. *Assume that, the total tolerable HWI of the $\mathcal{R}$ node is $k_R^t + k_R^r = k_R$. Furthermore, we assume the joint EVM constraint in the $\mathcal{S}$ and $\mathcal{D}$ nodes to be $k_S^t + k_D^r = k_{SD}$. The BLER floor $g(d_1, d_2)$ is minimized if $k_S^t = k_D^r = \frac{k_{SD}}{2}$ and $k_R^t = k_R^r = \frac{k_R}{2}$.*

Proof. Since $d_1 d_2 = d + 1$, we can rewrite the BLER floor term as a function of d as $g(d) = \frac{\beta_1\sigma_{e_{RD}}^2 + \beta_2\sigma_{e_{SR}}^2}{\beta_1\beta_2(1-\theta_m d)}(d+1)\theta_m$. Taking the derivative of g with respect to d reveals that $\frac{\partial g}{\partial d} > 0$, which means that g is a monotonically increasing function of d. So the minimum value of g will be obtained if d is minimized. The steps of minimizing d are presented in detail in Appendix C. This finally leads to the conditions of $k_S^t = k_D^r = \frac{k_{SD}}{2}$ and $k_R^t = k_R^r = \frac{k_R}{2}$.

In the above corollaries and through the rest of the paper, we mostly discuss the BLER and the associated minimization methods. In the following corollary, we also design the considered communication network from energy efficiency (EE) perspective. Toward this end, we will try to minimize the total SNR available to the system given a specific BLER constraint using the high-SNR expression in (47).

Corollary 5. *Assume that the maximum tolerable BLER is ϵ_t, implying that $\epsilon_{ave} < \epsilon_t$. Under this condition, the total normalized transmission power of the network will be minimized if*

$$\gamma_S = \frac{\theta_m}{1-\theta_m d}\sqrt{\frac{d_2}{\beta_1}}.\frac{\sqrt{\frac{d_1}{\beta_2}} + \sqrt{\frac{d_2}{\beta_1}}}{\epsilon_t - g(d_1, d_2)} \tag{49}$$

and

$$\gamma_R = \frac{\theta_m}{1-\theta_m d}\sqrt{\frac{d_1}{\beta_2}}.\frac{\sqrt{\frac{d_1}{\beta_2}} + \sqrt{\frac{d_2}{\beta_1}}}{\epsilon_t - g(d_1, d_2)}. \tag{50}$$

Additionally, the minimum total normalized transmission power required for satisfying the maximum tolerable BLER condition is

$$\gamma_{tot} = \frac{\theta_m}{1-\theta_m d}\frac{\left(\sqrt{\frac{d_1}{\beta_2}} + \sqrt{\frac{d_2}{\beta_1}}\right)^2}{\epsilon_t - g(d_1, d_2)}. \tag{51}$$

Proof. To address the EE strategy in this corollary, we have to solve the following optimization problem

$$\begin{aligned} minimize \quad & \gamma_T \\ s.t. \quad & \gamma_T = \gamma_S + \gamma_R, \\ & \epsilon_{ave} < \epsilon_t. \end{aligned} \tag{52}$$

To solve (52), we can use the classic Lagrange multiplier method. Using (47) will lead to

$$\mathcal{L}(\gamma_S, \gamma_R, \lambda) = \gamma_S + \gamma_R + \lambda\Big(\frac{d_2\theta_m}{\beta_1(1-\theta_m d)}.\frac{1}{\gamma_S} + \frac{d_1\theta_m}{\beta_2(1-\theta_m d)}.\frac{1}{\gamma_R} + g(d_1, d \tag{53}$$

Upon jointly solving the equations $\frac{\partial \mathcal{L}}{\partial \gamma_S} = 0$, $\frac{\partial \mathcal{L}}{\partial \gamma_R} = 0$ and $\frac{\partial \mathcal{L}}{\partial \lambda} = 0$, the expressions in (49), (50) and (51) will be obtained.

B. Asymptotic SNR Regime

In the previous section, we discussed the asymptotic average BLER both in the cases of perfect hardware and perfect channel estimation. Here, we intend to minimize the average BLER in both these cases subject to a total CEE and total EVM constraint, respectively.

1) Perfect Hardware: In this part, we consider the instantaneous SNDR expression of (44) and minimize the BLER as

a function of the CSI error in the two hops. To do this, we present the following corollary.

Corollary 6. *Assume the total CEE constraint to be* $\sigma^2_{e_{SR}} + \sigma^2_{e_{RD}} = \sigma^2_{e_{tot}}$. *The SNDR expression* (44) *is maximized if*

$$\begin{cases} \sigma^2_{e_{SR}} = 0 \quad , \quad \sigma^2_{e_{RD}} = \sigma^2_{e_{tot}} & |\hat{h}_{SR}|^2 < |\hat{h}_{RD}|^2 \\ \sigma^2_{e_{RD}} = 0 \quad , \quad \sigma^2_{e_{SR}} = \sigma^2_{e_{tot}} & |\hat{h}_{SR}|^2 > |\hat{h}_{RD}|^2 \end{cases}. \tag{54}$$

When we consider an arbitrary function $f(x)$ *and we define* $f_{\nu,\kappa} = f(\kappa) - f(\nu)$, *then the average BLER of a Nakagami-*m *channel relying on adaptive-duration training can be expressed as*

$$\epsilon^{\infty}_{ave} = 1 + \Psi_{\psi,\omega} + \Xi_{\omega,\psi}, \tag{55}$$

where $\Psi(x)$ *and* $\Xi(x)$ *are defined at the top of the next page.*

Proof. Please see Appendix D.

Corollary 6. suggests that for maximizing the instantaneous SNDR, the total CEE of the hops should be shared in line with the current status of the two channels. According to (39) and (40), this can be arranged by appropriately adjusting the training power and training duration of each hop. This is termed here as "adaptive-duration training", which is a well-known technique of enhancing the robustness of a wireless system [44].

2) Perfect Channel State Information: In this part, we consider the average BLER expression of (45). This expression shows that transceiver impairments can dramatically degrade the AF relaying performance and should be taken into account when designing the system. To this end, we assume having a joint total EVM constraint in the $\mathcal{S}$ and $\mathcal{D}$ nodes in addition to another EVM constraint only related to the $\mathcal{R}$ node.

Corollary 7. *Assume that the total tolerable HWI of the* $\mathcal{R}$ *node is* $k^t_R + k^r_R = k_R$. *Furthermore, we assume the joint EVM constraint in the* $\mathcal{S}$ *and* $\mathcal{D}$ *nodes to be* $k^t_S + k^r_D = k_{SD}$. *The average BLER is minimized if* $k^t_S = k^r_D = \frac{k_{SD}}{2}$ *and* $k^t_R = k^r_R = \frac{k_R}{2}$.

Proof. As $Q(\frac{1}{d})$ is a monotonically decreasing function of $\frac{1}{d}$, to minimize the average BLER, $\frac{1}{d}$ should be maximized or equivalently d should be minimized. The steps of minimizing d are presented in detail in Appendix C, which finally leads to the conditions $k^t_S = k^r_D = \frac{k_{SD}}{2}$ and $k^t_R = k^r_R = \frac{k_R}{2}$.

We note that according to the above corollary, having the same hardware quality in the $\mathcal{S}$ and $\mathcal{D}$ nodes is better than having a high-quality and a low-quality node. Furthermore, the maximum tolerable HWI in $\mathcal{R}$ should be equally distributed among the transmit and receive front-ends.

Here, we highlight that the level of HWIs directly depends on the quality of hardware utilized in RF section of the nodes. In designing low-cost IoT relaying networks, these inevitable impairments may become particularly grave [18]. As such, the financial budget and revenue for implementing the network will eventually determine the total tolerable HWIs. Equivalently, the HWI allocation can be interpreted as the total revenue dedicated to the nodes involved. Thus, the optimization result can be exploited at the design stage of the system.

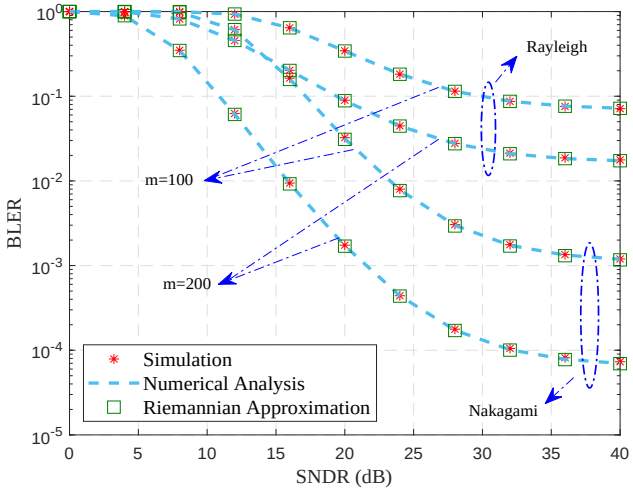

Fig. 3: Riemannian approximation of (25) and numerical method for (23).

VII. Numerical Results and Discussions

In this section we discuss and analyze the exact and approximate results derived in the previous sections for the average BLER and will validate their accuracy by Monte Carlo simulations. In the simulations, we assume $\gamma_S = \gamma_R$, $\hat{m} = 1000$, $N = 256$, $\mathbb{E}\{h^2_{SR}\} = \mathbb{E}\{h^2_{RD}\} = 1$, unless otherwise stated.

Fig. 3 shows the average BLER versus SNR for different values of m in Nakagami-m and Rayleigh fading channels. In Section III we stated that deriving an exact analytical expression for the general case of our scenario through solving the integral in (23) is not feasible and requires a numerical solution. Accordingly, the Riemannian approximation of (25) was proposed. This figure shows a very good match between the proposed approximate expression as well as the numerical and simulation results. We note that even for the low values of m as $m = 100$, the approximation is tight for both the Nakagami-m and Rayleigh channels. This shows that the Riemannian approximation is a useful tool when the integrand in (23) has a complex form for various wireless channels.

Fig. 4 validates our expressions in (32) and (35) for the average BLER of the imperfect hardware and imperfect CSI cases, respectively. As a benchmark, the results of the perfect hardware-CSI scenario are also depicted in the figure, where the analytical result is derived through setting $\alpha_0 = 0$ in (35). This will reproduce the result given in [12, eq. 6], which is a special case of our imperfect CSI scenario. To reproduce this result, k and n in (35) are set to 2, and j is set to zero. This yields a perfect match between the simulation and analytical results for this case. For the case of perfect hardware associated with CEE, the analytical results are plotted through setting $k = 2$, $j = 6$, $n = 2$ in (35), which again produces a good match between our simulations and theory for this case. Here, the truncation error is dependent of the CEE level, hence upon reducing the CEE variances, we will need more terms to reproduce the floor effect in the series. However, in this figure, the CEE variances are set to very low values,

$$\Psi(x) = \sum_{k_1=0}^{m_1-1} \sum_{i=0}^{k_1} \frac{x^{k_1-i}\sigma_{e_{tot}}^{2^{k_1-i-1}}}{(k_1-i)!\ \theta_1^{k_1-i-1}} e^{-\frac{x\sigma_{e_{tot}}^2}{\theta_1}} + \sum_{k_2=0}^{m_2-1} \sum_{j=0}^{k_2} \frac{x^{k_2-j}\sigma_{e_{tot}}^{2^{k_2-j-1}}}{(k_2-j)!\ \theta_2^{k_2-j-1}} e^{-\frac{x\sigma_{e_{tot}}^2}{\theta_2}}, \tag{56}$$

$$\Xi(x) = \sum_{k_1=0}^{m_1-1} \sum_{k_2=0}^{m_2-1} \sum_{k=0}^{k_1+k_2} \frac{k! x^{k_1+k_2-k}\sigma_{e_{tot}}^{2^{k_1+k_2-k-1}}}{k_1!k_2!\theta_1^{k_1}\theta_2^{k_2}} \left(\frac{\theta_1\theta_2}{\theta_1+\theta_2}\right)^{k+1} \binom{k_1+k_2}{k} e^{-x(\frac{1}{\theta_1}+\frac{1}{\theta_2})\sigma_{e_{tot}}^2}, \tag{57}$$

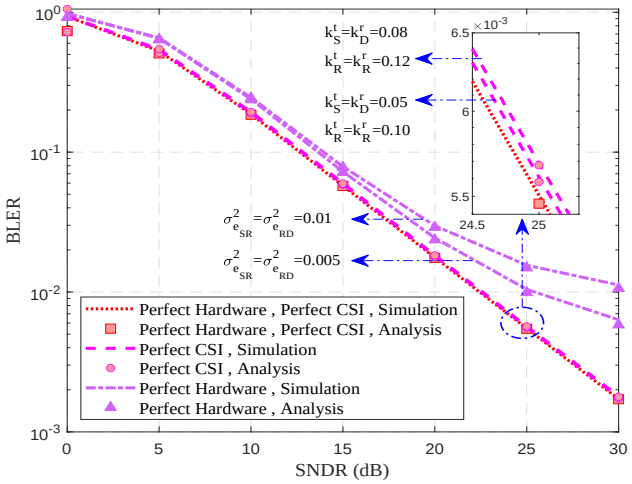

Fig. 4: BLER vs SNDR for Perfect Hardware in (35) and Perfect CSI in (32) in Rayleigh channel.

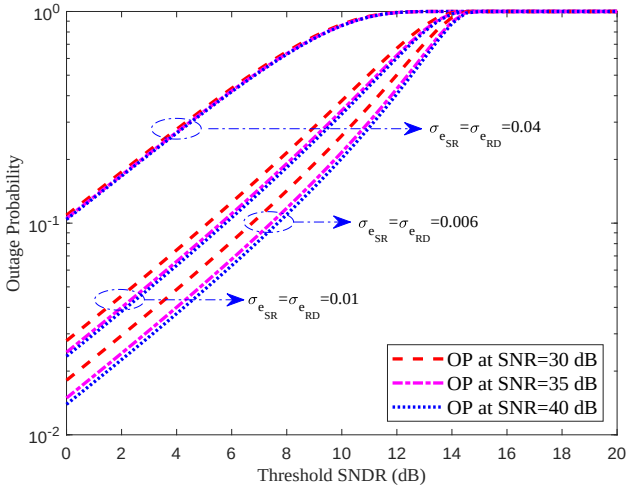

Fig. 5: visualization of CEE Effects: OP vs SNDR based on (18)

hence resulting in the worst case for the associated truncation error. Hence in practical scenarios, there will be no need to consider more terms. Furthermore, for the perfect CSI with HWI, the analytical results are plotted by setting $i = 4$ and $n = 2$ in (32). Again the figure shows that the truncation error is negligible and a perfect match is seen. Here, the truncation error depends both on the SNDR and on the level of impairments, hence upon increasing the SNDR and HWI the truncation error will be aggravated. However, in Fig. 4, we have plotted the curves of this case for the high-SDNR regime and for the maximum levels of HWIs found in the related literature [18], [41]. This can be interpreted that we have considered the worst-case of truncation error and there is no need to increase the number of terms in a practical scenario. Additionally, the figure shows that the degradation of the average BLER for the perfect hardware scenario is more serious than the case of the perfect CSI. This is due to the floor formation caused by CEE, which has a more grave effect than the error floor caused by HWIs.

To get further insights concerning the impact of imperfect CSI, Fig. 5 shows the outage probability (OP) for our scenario in a Rayleigh channel based on the expression in (18). Three group of curves are plotted, each for different values of CEE variances for the high SNR values of 30, 35 and 40 dB. As shown in the figure, by increasing the CEE variance, the related high-SNR curves merge at 100% OP. Explicitly, the system is always in outage for large values of $\sigma^2_{e_{SR}}$ and $\sigma^2_{e_{RD}}$ according to (23). The average BLER may be determined by

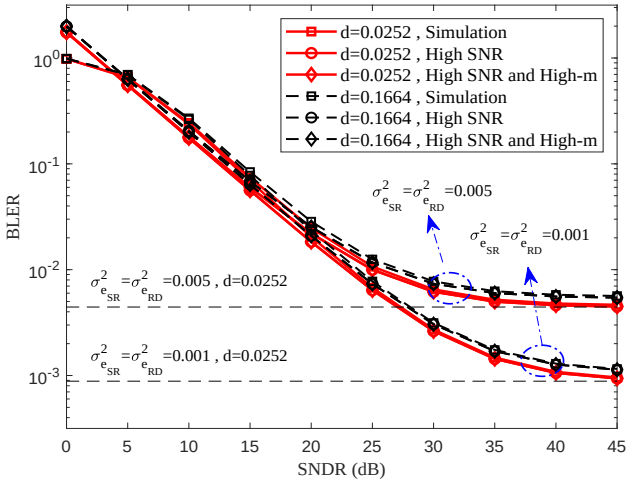

Fig. 6: BLER vs SNDR for High-Power and High-m approximations in equations (38) and (43).

integrating these curves.

It is shown in Fig. 6 that our expressions derived for the high-SNR regime for the Rayleigh channels is tight, regardless of the value of m. This observation is vital, as the exact expressions derived for the average BLER failed to give clear practical insights into the problem, including those obtained through using the Riemannian approximation. In this figure, the expressions (38) and (43) are compared to the simulation

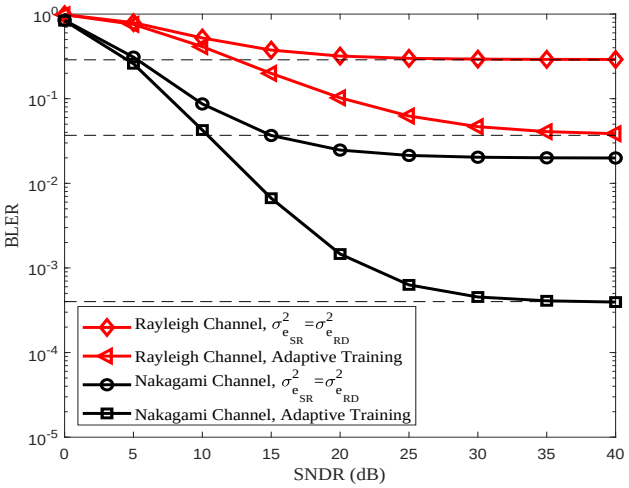

Fig. 7: BLER vs SNDR for Using Adaptive-Duration Training for Perfect Hardware.

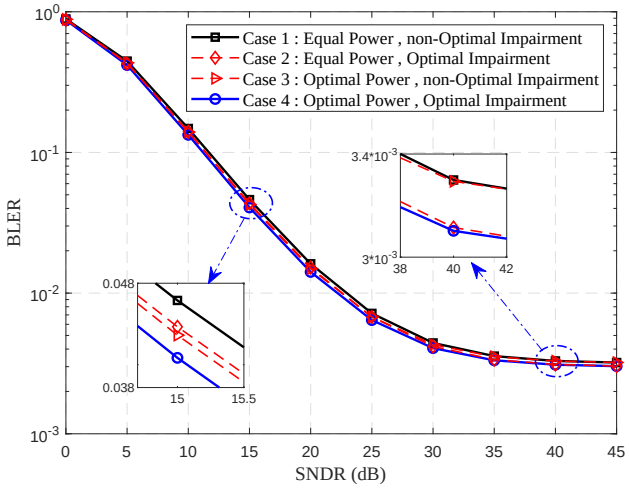

Fig. 8: BLER vs SNDR relying on Power Allocation and Efficient Impairment Distribution.

results by considering two different values of CEE variances namely $\sigma^2_{e_{SR}} = \sigma^2_{e_{RD}} = 0.005$ and $\sigma^2_{e_{SR}} = \sigma^2_{e_{RD}} = 0.001$ and also a pair of different total impairment levels of $d = 0.0252$ and $d = 0.1664$. This figure shows that the dominant error floor effect is due to the CEE. However, the level of total impairment d further degrades the deletion effect of a high CEE variance. We also note that the expression in (43) represents a very tight approximation for high SNRs, just like (38). Given its simplicity and tightness, we use it for our further analysis in the optimization problem, rather than using the more complex expression of (38).

In Fig. 7 our proposed adaptive-duration training scheme is compared for the case of perfect hardware to the equally distributed CEE level used in both hops. The following considerations should be taken into account : 1) the proposed scheme is not limited to a specific fading channel, it can be readily used for any wireless channels. Here both the Rayleigh and Nakagami-m channels are investigated. 2) The proposed scheme is not limited to low CEEs. In this figure the CEE levels are considered to be $\sigma^2_{e_{SR}} = \sigma^2_{e_{RD}} = 0.2$. According to the simulation results, our proposed scheme significantly enhances the average BLER performance of the short-packet system for both Rayleigh and Nakagami-m channels. This is an important observation, since we discussed in Fig 4. that the effect of even very low CEEs lead to severely degraded average BLER. Fortunately, the adaptive-duration training scheme substantially mitigates the effect of CEE. The asymptotic expression derived in (55) is also plotted in the figure.

In Fig. 8, our proposed hardware design and power allocation schemes are studied. In this figure, the CEE variances are set to $\sigma^2_{e_{SR}} = \sigma^2_{e_{RD}} = 0.005$, while the impairment levels are assumed to be $k^t_S + k^r_D = 0.2$ and $k^t_R + k^r_R = 0.3$. Furthermore, we have assumed $\beta_1 = 4\beta_2$. Four cases are considered here regarding the power allocation and hardware design. As expected, 4 in which the power is optimally allocated and the hardware design is optimal outperforms the other

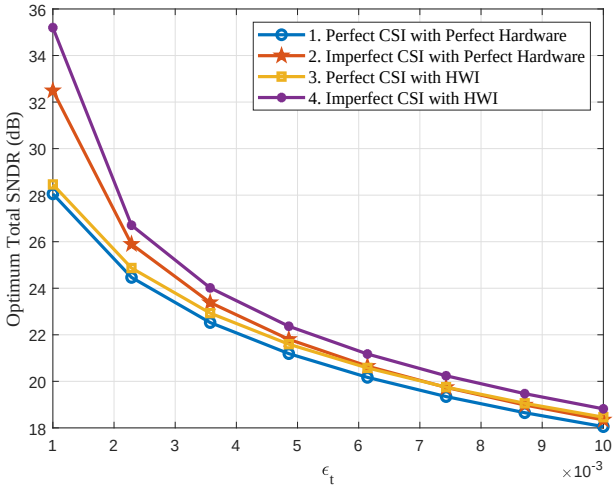

Fig. 9: Optimum total normalized transmission power vs target BLER for various CSI and HWI conditions.

three cases for the whole range of SNRs. In minimizing the average BLER, the following considerations should be taken into account : 1) The hardware cost of the relay node and also the joint cost of the hardware of the source and destination nodes, should be equally divided between the transmission and reception RF front ends. 2) The power sharing between the source and relay depends on the level of impairments in the two hops. According to Corollary 3, if we increase the impairment level in the first hop, the power allocated to the source node should be decreased. This is because increasing the power of nodes in a link having a considerable level of HWIs does not necessarily improve the BLER performance. For instance, when using a non-linear power amplifier, although increasing the output power will improve the message signal, it will also lead to higher distortion at the output. Thus the power in such systems has to be allocated bearing in mind the level of impairment present in them.

In Fig. 9, the optimum total normalized transmission power expression in (51) is plotted for $\sigma^2_{e_{SR}} = 0.001$, $\sigma^2_{e_{RD}} = 0.001$, $d_1 = 1.08$, $d_2 = 1.08$ and $r = 0.4$. Firstly, the perfect hardware and perfect CSI scenario is used as our benchmark and it is contrasted to the scenarios associated with the imperfect cases. At low target BLERs, our benchmark performs close to the perfect CSI scenario associated with HWIs. However, when realistic CSI imperfections are imposed, a significant performance gap is introduced compared to the idealized perfect scenario and this gap is further aggravated by the presence of HWIs, as shown in the fourth scenario of Fig. 9. We also note that the curves associated with the second and third scenarios exhibit a cross over. In a nutshell, it depends on the target BLERs, which of these scenarios is the most power-efficient. Consequently, the point in which the curves of the latter scenarios cross over depends on the BLER floor level which is itself mainly determined by the CSI imperfection. Accordingly, we note that by properly adjusting the impairment levels in nodes similar to our approach in Corollary 4, we can minimize the BLER floor term and get better results in terms of EE. Finally, Fig. 9 clearly illustrates that the realistic imperfections considered tend to have a grave impact on the EE of a cooperative SPC system.

VIII. Conclusions

We considered an AF relaying system and examined the average BLER performance of this system in the presence of realistic HWIs and CEEs. We derived the outage probability of this system for Nakagami fading channels. Then, we obtained the approximate expression of the average BLER using the Riemannian approximation and showed that the resultant expression is tight even when the block-length is as low as 100. At the next step, novel closed-form expressions were derived for a Rayleigh fading channel for the two cases, namely for perfect CEE with HWI and perfect hardware with CEE. The latter exact analysis along with the former Riemannian approximate BLER, are useful in low SNR scenarios which might be quite common in IoT applications. Furthermore, simplified high-SNR and asymptotic-SNR expressions were derived and several optimization problems were solved for minimizing the average BLER and total power. Our numerical results showed that the CEE can result in a significant performance loss by introducing BLER floor even if it has a very low value. We also observed that significant HWIs can lead to an excessive BLER. Additionally, both the CEEs and HWIs degrade the energy efficiency compared to the idealized perfect-CSI and perfect-hardware scenario. Finally, our numerical results showed that the proposed adaptive-duration training method can significantly enhance the average BLER performance in a perfect hardware scenario, despite having non-negligible CEE.

Appendix A

In (9) if we define $X_1 = |h_{SR}|^2$ and $X_2 = |h_{RD}|^2$, we can write

$$Pr(\gamma < \gamma_{th}) = 1 - Pr\Big(X_2 > \frac{\alpha_3\gamma_{th}X_1 + \alpha_0\gamma_{th}}{(\alpha_1 - \alpha_2\gamma_{th})X_1 - \alpha_4\gamma_{th}}\Big) = \begin{cases} 1 - g(\gamma_{th}), & \gamma_{\rm th} < \frac{\alpha_1}{\alpha_2} \\ 1, & \gamma_{\rm th} > \frac{\alpha_1}{\alpha_2} \end{cases}, \tag{58}$$

where, $g(\gamma_{th}) = Pr\Big(X_2 > \frac{\alpha_3\gamma_{th}X_1+\alpha_0\gamma_{th}}{(\alpha_1-\alpha_2\gamma_{th})X_1-\alpha_4\gamma_{th}}\Big)$, if $\gamma_{\rm th} < \frac{\alpha_1}{\alpha_2}$. By defining $p(X_1) = \frac{\alpha_3\gamma_{th}X_1+\alpha_0\gamma_{th}}{(\alpha_1-\alpha_2\gamma_{th})X_1-\alpha_4\gamma_{th}}$ and $X_{1_\infty} = \frac{\alpha_4\gamma_{th}}{\alpha_1-\alpha_2\gamma_{th}}$ we have to solve the following integrals

$$g(\gamma_{th}) = \int_{X_{1_\infty}}^{\infty} f_{X_1}(x_1) \int_{p(X_1)}^{\infty} f_{X_2}(x_2) dx_2 dx_1, \tag{59}$$

where $f_{X_1}(x_1)$ and $f_{X_2}(x_2)$ obey the distribution described by (15). By applying [45, eq. 2.32-2], (59) can be written as

$$g(\gamma_{th}) = \sum_{k=0}^{m_2-1} \frac{\theta_2^{k+1} k! \binom{m_2-1}{k}}{\Gamma(m_1)\Gamma(m_2)\theta_1^{m_1}\theta_2^{m_2}} \times \int_{X_{1_\infty}}^{\infty} x_1^{m_1-1} \Big(p(x_1)\Big)^{m_2-1-k} e^{-\frac{x_1}{\theta_1} - \frac{p(x_1)}{\theta_2}} dx_1. \tag{60}$$

By changing variables $u = (\alpha_1 - \alpha_2\gamma_{th})x_1 - \alpha_4\gamma_{th}$, and by defining $\phi_1 = \alpha_4\gamma_{th}$, $\phi_2 = \alpha_1 - \alpha_2\gamma_{th}$, $\phi_3 = \frac{\alpha_3\gamma_{th}}{\alpha_1-\alpha_2\gamma_{th}}$ and $\phi_4 = \alpha_0\gamma_{th} + \frac{\alpha_3\alpha_4\gamma_{th}^2}{\alpha_1-\alpha_2\gamma_{th}}$, the expression in (60) can be written as

$$g(\gamma_{th}) = \sum_{k=0}^{m_2-1} \frac{\theta_2^{k+1} k! \binom{m_2-1}{k}}{\Gamma(m_1)\Gamma(m_2)\theta_1^{m_1}\theta_2^{m_2}} \frac{\exp\Big(-\frac{\phi_1}{\theta_1\phi_2} - \frac{\phi_3}{\theta_2}\Big)\phi_3^m}{\phi_2^{n+1}} \int_0^{\infty} \frac{\Big(u+\phi_1\Big)^n \Big(u+\frac{\phi_4}{\phi_3}\Big)^m}{u^m} \exp\Big(-\frac{1}{\theta_1\phi_2}u - \frac{\phi_4}{\theta_2}\frac{1}{u}\Big) du, \tag{61}$$

where, $n = m_1 - 1$ and $m = m_2 - 1 - k$. Applying the binomial expansion to the integrands in (61) and using [45, eq. 3.471-9] will lead to the final expression for $g(\gamma_{th})$

$$g(\gamma_{th}) = \frac{2\exp\Big(-\frac{\phi_1}{\theta_1\phi_2} - \frac{\phi_3}{\theta_2}\Big)\phi_3^{m_2-1}}{\Gamma(m_1)\Gamma(m_2)\theta_1^{m_1}\theta_2^{m_2}\phi_2^{m_1}} \sum_{k=0}^{m_2-1} \sum_{i=0}^{m_1-1} \sum_{j=0}^{m_2-k-1} k! \binom{m_2-1}{k} \binom{m_1-1}{i} \binom{m_2-k-1}{j} \theta_2^{k+1} \phi_1^{m_1-i-1} \phi_3^{-k} \Big(\frac{\phi_4}{\phi_3}\Big)^j \Big(\frac{\theta_1\phi_2\phi_4}{\theta_2}\Big)^{\frac{i-j+1}{2}} . K_{i-j+1}\Big(2\sqrt{\frac{\phi_4}{\phi_2\theta_1\theta_2}}\Big). \tag{62}$$

Appendix B

By inserting (33) into (23) we obtain

$$\epsilon_{ave} \approx 1 - \sqrt{\frac{2}{\pi}} \frac{\alpha_m}{\beta_1\alpha_1} \int_{\psi}^{\omega} e^{-\frac{\beta_2\alpha_4+\beta_1\alpha_3}{\beta_1\beta_2\alpha_1}x} \sqrt{\frac{\alpha_3\alpha_4x^2 + \alpha_0\alpha_1x}{\beta_2}} \beta_1 . K_1\left(\frac{2}{\alpha_1}\sqrt{\frac{\alpha_3\alpha_4x^2 + \alpha_0\alpha_1x}{\beta_1\beta_2}}\right) dx. \tag{63}$$

Using a series representation for $e^{-\frac{\beta_2\alpha_4+\beta_1\alpha_3}{\beta_1\beta_2\alpha_1}x} = \sum_{k=0}^{\infty}\frac{(-1)^k}{k!}(\frac{\beta_2\alpha_4+\beta_1\alpha_3}{\beta_1\beta_2\alpha_1})^k x^k$ will lead to

$$\epsilon_{ave} \approx 1-\sqrt{\frac{2}{\pi}}\frac{\alpha_m}{\beta_1\alpha_1}\sum_{k=0}^{\infty}\frac{(-1)^k}{k!}\Big(\frac{\beta_2\alpha_4+\beta_1\alpha_3}{\beta_1\beta_2\alpha_1}\Big)^k \int_{\psi}^{\omega} x^k\sqrt{\frac{\alpha_3\alpha_4x^2+\alpha_0\alpha_1x}{\beta_2}}\beta_1.K_1\left(\frac{2}{\alpha_1}\sqrt{\frac{\alpha_3\alpha_4x^2+\alpha_0\alpha_1x}{\beta_1\beta_2}}\right)dx.$$

By changing variables as $h(x)=\frac{2}{\alpha_1}\sqrt{\frac{\alpha_3\alpha_4x^2+\alpha_0\alpha_1x}{\beta_1\beta_2}}$ we can write

$$\epsilon_{ave} \approx 1-\frac{\alpha_m}{\sqrt{2\pi}}\frac{\alpha_1\beta_1\beta_2}{2}\sum_{k=0}^{\infty}\frac{(-1)^k}{k!}\Big(\frac{\beta_2\alpha_4+\beta_1\alpha_3}{2\beta_1\beta_2\alpha_1\alpha_3\alpha_4}\Big)^k \int_{h(\psi)}^{h(\omega)}\frac{(\sqrt{\alpha_0^2\alpha_1^2+\alpha_3\alpha_4\alpha_1^2\beta_1\beta_2h^2}-\alpha_0\alpha_1)^k}{\sqrt{\alpha_0^2+\alpha_3\alpha_4\beta_1\beta_2h^2}}h^2K_1(h)dh. \tag{64}$$

Using the binomial expansion for $\big(\sqrt{\alpha_0^2\alpha_1^2+\alpha_3\alpha_4\alpha_1^2\beta_1\beta_2h^2}-\alpha_0\alpha_1\big)^k$ will lead to

$$\epsilon_{ave} \approx 1-\frac{\alpha_m}{\sqrt{2\pi}}\frac{\alpha_1\beta_1\beta_2}{2}\sum_{k=0}^{\infty}\sum_{i=0}^{k}\frac{(-1)^k}{k!}\Big(\frac{\beta_2\alpha_4+\beta_1\alpha_3}{2\beta_1\beta_2\alpha_1\alpha_3\alpha_4}\Big)^k \binom{k}{i}\alpha_1^i(-\alpha_0\alpha_1)^{k-i}\int_{h(\psi)}^{h(\omega)}(\alpha_0^2+\alpha_3\alpha_4\beta_1\beta_2h^2)^{\frac{i-1}{2}}h^2K_1(h)dh. \tag{65}$$

Finally, using the binomial expansion for $(\alpha_0^2+\alpha_3\alpha_4\beta_1\beta_2h^2)^{\frac{i-1}{2}}=\sum_{j=0}^{\infty}\frac{\Gamma(q+1)}{\Gamma(q-j+1)j!}(\alpha_3\alpha_4\beta_1\beta_2h^2)^{q-j}(\alpha_0^2)^j$ will lead to (34), where $q=\frac{i-1}{2}$.

APPENDIX C

Let us substitute $k_D^r = k_{SD}-k_S^t$ and $k_R^r=k_R-k_R^t$ into d. This will lead to

$$d=\Big[{k_R^t}^2+(k_{SD}-k_S^t)^2\Big]\Big[1+{k_S^t}^2+(k_R-k_R^t)^2\Big]+{k_S^t}^2+(k_R-k_R^t)^2. \tag{66}$$

Now, we evaluate $\frac{\partial d}{\partial k_S^t}$ as well as $\frac{\partial d}{\partial k_R^t}$ and set them equal to zero, leading to

$$\frac{\partial d}{\partial k_S^t} = -\Big[1+{k_S^t}^2+(k_R-k_R^t)^2\Big](k_{SD}-k_S^t) + k_S^t\Big[1+{k_R^t}^2+(k_{SD}-k_S^t)^2\Big]=0, \tag{67}$$

$$\frac{\partial d}{\partial k_R^t} = -(k_R-k_R^t)\Big[1+{k_R^t}^2+(k_{SD}-k_S^t)^2\Big] + \Big[1+{k_S^t}^2+(k_R-k_R^t)^2\Big]k_R^t=0. \tag{68}$$

Comparing (67) and (68), one can infer $k_Rk_S^t+k_{SD}k_R^t=k_Rk_{SD}$. Substituting this into (67) and (68) will lead to the following third-order equations for optimum values of k_S^t and k_R^t.

$$2(k_{SD}^2+k_R^2){k_S^t}^3-3k_{SD}(k_{SD}^2+k_R^2){k_S^t}^2 + k_{SD}^2(k_{SD}^2+k_R^2+2)k_S^t-k_{SD}^3=0, \tag{69}$$

$$2(k_{SD}^2+k_R^2){k_R^t}^3-3k_R(k_{SD}^2+k_R^2){k_R^t}^2 + k_R^2(k_{SD}^2+k_R^2+2)k_R^t-k_R^3=0. \tag{70}$$

Substituting $k_S^t=\frac{k_{SD}}{2}$ and $k_R^t=\frac{k_R}{2}$ into (69) and (70), respectively, unveils that these values are the roots of the above equations. We note that (69) and (70) have a single real root and two non-real complex conjugate roots. So the only solution for these equations are $k_S^t=\frac{k_{SD}}{2}$ and $k_R^t=\frac{k_R}{2}$, respectively.

APPENDIX D

For maximizing the instantaneous SNDR in (44), we can alternatively minimize the expression below

$$\mu=\sigma_{e_{RD}}^2|\hat{h}_{SR}|^2+\sigma_{e_{SR}}^2|\hat{h}_{RD}|^2+\sigma_{e_{SR}}^2\sigma_{e_{RD}}^2. \tag{71}$$

By substituting $\sigma_{e_{RD}}^2=\sigma_{e_{tot}}^2-\sigma_{e_{SR}}^2$ into μ of (71) and calculating the second derivative with respect to $\sigma_{e_{SR}}^2$, we can find that $\frac{\partial\mu}{\partial\sigma_{e_{SR}}^2}<0$. Thus, μ is a concave function with respect to $\sigma_{e_{SR}}^2$ and it is minimized in the boundaries 0 and $\sigma_{e_{tot}}^2$,

$$\mu(\sigma_{e_{SR}}^2=0)=\sigma_{e_{tot}}^2|\hat{h}_{SR}|^2 \tag{72}$$

$$\mu(\sigma_{e_{SR}}^2=\sigma_{e_{tot}}^2)=\sigma_{e_{tot}}^2|\hat{h}_{RD}|^2. \tag{73}$$

Any of the above values which are less than the other, will determine the optimum $\sigma_{e_{SR}}^2$ and $\sigma_{e_{RD}}^2$. This is expressed in (54).

To calculate the average BLER we first rewrite the maximized SNDR expression as

$$\gamma_{SD_\infty}^{max}=\frac{max(|\hat{h}_{SR}|^2,|\hat{h}_{RD}|^2)}{\sigma_{e_{tot}}^2}. \tag{74}$$

Since we have assumed a Nakagami-m fading channel, $|\hat{h}_{SR}|^2$ and $|\hat{h}_{RD}|^2$ have gamma distribution, with their CDFs defined in (15). So the CDF of the maximized SNDR can be written as

$$F_{\gamma_{SD_\infty}^{max}}(x) = 1-\sum_{k_1=0}^{m_1-1}\frac{\sigma_{e_{tot}}^{2k_1}x^{k_1}}{k_1!\theta_1^{k_1}}e^{-\frac{x\sigma_{e_{tot}}^2}{\theta_1}}-\sum_{k_2=0}^{m_2-1}\frac{\sigma_{e_{tot}}^{2k_2}x^{k_2}}{k_2!\theta_2^{k_2}}e^{-\frac{x\sigma_{e_{tot}}^2}{\theta_2}} \sum_{k_1=0}^{m_1-1}\sum_{k_2=0}^{m_2-1}\frac{\sigma_{e_{tot}}^{2(k_1+k_2)}x^{k_1+k_2}}{k_1!k_2!\theta_1^{k_1}\theta_2^{k_2}}e^{-x\sigma_{e_{tot}}^2(\frac{1}{\theta_1}+\frac{1}{\theta_2})}. \tag{75}$$

Substituting (75) into (23), after some further manipulations, will arrive at the average BLER in (55).

REFERENCES

[1] L. Zhang and Y. Liang, "Average throughput analysis and optimization in cooperative IoT networks with short packet communication," *IEEE Trans. Veh. Technol.*, vol. 67, no. 12, pp. 11549-11562, Dec. 2018.

[2] M. Letafati, A. Kuhestani, K. -K. Wong and M. J. Piran, "A lightweight secure and resilient transmission scheme for the Internet-of-Things in the presence of a hostile jammer," *IEEE Internet of Things J.*, doi: 10.1109/JIOT.2020.3026475.

[3] S. Jain and R. Bose, "Rateless-code-based secure cooperative transmission scheme for industrial IoT," *IEEE Internet of Things J.*, vol. 7, no. 7, pp. 6550-6565, July 2020, doi: 10.1109/JIOT.2020.2969955.

[4] P. Schulz, M. Matthe, H. Klessig, M. Simsek, G. Fettweis, J. Ansari, S. A. Ashraf, B. Almeroth, J. Voigt, I. Riedel, A. Puschmann, A. Mitschele-Thiel, M. Muller, T. Elste, M. Windisch, "Latency critical IoT applications in 5G: Perspective on the design of radio interface and network architecture," *IEEE Commun. Mag.*, vol. 55, no. 2, pp. 70-78, Feb. 2017.

[5] Y. Polyanskiy, H. V. Poor and S. Verdu, "Channel coding rate in the finite blocklength regime," *IEEE Trans. Inf. Theory*, vol. 56, no. 5, pp. 2307-2359, May 2010.

[6] T. Hou, Y. Liu, Z. Song, X. Sun and Y. Chen, "NOMA-enhanced terrestrial and aerial IoT networks with partial CSI," *IEEE Internet of Things J.*, vol. 7, no. 4, pp. 3254-3266, April 2020.

[7] W. Yang, G. Durisi, T. Koch and Y. Polyanskiy, "Quasi-static multiple-antenna fading channels at finite blocklength," *IEEE Trans. Inf. Theory*, vol. 60, no. 7, pp. 4232-4265, July 2014.

[8] C. Li, N. Yang and S. Yan, "Optimal transmission of short-packet communications in multiple-input single-output systems," *IEEE Trans. Veh. Technol.*, vol. 68, no. 7, pp. 7199-7203, July 2019.

[9] Y. Hu, A. Schmeink and J. Gross, "Blocklength-limited performance of relaying under quasi-static Rayleigh channels," *IEEE Trans. Wireless Commun.*, vol. 15, no. 7, pp. 4548-4558, July 2016.

[10] Y. Gu, H. Chen, Y. Li and B. Vucetic, "Ultra-reliable short-packet communications: half-duplex or full-duplex relaying?," *IEEE Wireless Commun. Lett.*, vol. 7, no. 3, pp. 348-351, June 2018.

[11] X. Lai, Q. Zhang and J. Qin, "Cooperative NOMA short-packet communications in flat Rayleigh fading channels," *IEEE Trans. Veh. Technol*, vol. 68, no. 6, pp. 6182-6186, June 2019.

[12] Y. Gu, H. Chen, Y. Li, L. Song and B. Vucetic, "Short-packet two-way amplify-and-forward relaying," *IEEE Signal Process. Lett.*, vol. 25, no. 2, pp. 263-267, Feb. 2018.

[13] Y. Yang, Y. Song and F. Cao, "HARQ assisted short-packet communications for cooperative networks over Nakagami-m fading channels," *IEEE Access*, vol. 8, pp. 151171-151179, Feb. 2020.

[14] E. Costa and S. Pupolin, "M-QAM-OFDM system performance in the presence of a nonlinear amplifier and phase noise," *IEEE Trans. on Commun.*, vol. 50, no. 3, pp. 462-472, March 2002, doi: 10.1109/26.990908.

[15] T. Schenk, "RF imperfections in high-rate wireless systems: Impact and digital compensation". Dordrecht, The Netherlands: Springer, 2008.

[16] C. Studer, M. Wenk, and A. Burg, "MIMO transmission with residual transmit-RF impairments," in *Proc. ITG/IEEE Workshop Smart Antennas*, Feb. 2010, pp. 189196.

[17] M. Letafati, A. Kuhestani and H. Behroozi, "Three-hop untrusted relay networks with hardware imperfections and channel estimation errors for Internet of things," *IEEE Trans. Inf. Forens. Sec.*, vol. 15, pp. 2856-2868, Mar. 2020.

[18] M. Moradikia, H. Bastami, A. Kuhestani, H. Behroozi and L. Hanzo, "Cooperative secure transmission relying on optimal power allocation in the presence of untrusted relays, a passive eavesdropper and hardware impairments," *IEEE Access*, vol. 7, pp. 116942-116964, Aug. 2019.

[19] A. Kuhestani, A. Mohammadi, K.-K. Wong, P. L. Yeoh, M. Moradikia, and M. R. A. Khandaker, Optimal power allocation by imperfect hardware analysis in untrusted relaying networks, *IEEE Trans. Wireless Commun.*, vol. 17, no. 7, pp. 4302–4314, July 2018.

[20] Z. Yan, B. Ouyang, X. Zhang and H. Liu, "Secrecy outage performance of opportunistic relay selection with limited CSI feedback," in *IEEE Wireless Commun. Lett.*, vol. 8, no. 6, pp. 1626-1630, Dec. 2019.

[21] N. I. Miridakis, T. A. Tsiftsis and H. Wang, "Zero forcing detection for short packet transmission under channel estimation errors," *IEEE Trans. Veh. Technol.*, vol. 68, no. 7, pp. 7164-7168, July 2019.

[22] S. Schiessl, H. Al-Zubaidy, M. Skoglund and J. Gross, "Delay performance of wireless communications with imperfect CSI and finite-length coding," *IEEE Trans. Commun.*, vol. 66, no. 12, pp. 6527-6541, Dec. 2018.

[23] Y. Hu, A. Schmeink and J. Gross, "Optimal scheduling of reliability-constrained relaying system under Outdated CSI in the finite blocklength regime," *IEEE Trans. Veh. Technol.*, vol. 67, no. 7, pp. 6146-6155, July 2018, doi: 10.1109/TVT.2018.2811943.

[24] J. Zeng, T. Lv, R. P. Liu, X. Su, Y. J. Guo and N. C. Beaulieu, "Enabling ultrareliable and low-latency communications under shadow fading by massive MU-MIMO," *IEEE Internet Things J.*, vol. 7, no. 1, pp. 234-246, Jan. 2020.

[25] J. Wang, C. Jiang, H. Zhang, Y. Ren, K. -C. Chen and L. Hanzo, "Thirty Years of Machine Learning: The Road to Pareto-Optimal Wireless Networks," *IEEE Commun. Surveys Tuts.*, vol. 22, no. 3, pp. 1472-1514, thirdquarter 2020, doi: 10.1109/COMST.2020.2965856.

[26] J. Chen, H. Chen, H. Zhang and F. Zhao, "Spectral-energy efficiency tradeoff in relay-aided massive MIMO cellular networks with pilot contamination," *IEEE Access*, vol. 4, pp. 5234-5242, 2016.

[27] Z. Yan, B. Ouyang, X. Zhang and H. Liu, "Secrecy Outage performance of Opportunistic relay selection with limited CSI feedback," *IEEE Wireless Commun. Lett.*, vol. 8, no. 6, pp. 1626-1630, Dec. 2019.

[28] Y. Ma and J. Jin, Effect of channel estimation errors on M-QAM with MRC and EGC in Nakagami fading channels, *IEEE Trans. Veh.Technol.*, vol. 56, no. 3, pp. 12391250, May 2007.

[29] H. Xu and L. Sun, Encryption over the air: Securing two-way untrusted relaying systems through constellation overlapping, *IEEE Trans. Wireless Commun.*, vol. 17, no. 12, pp. 82688282, Dec. 2018.

[30] Z. Yang, Z. Ding, P. Fan, and G. K. Karagiannidis, On the performance of non-orthogonal multiple access systems with partial channel information, *IEEE Trans. Commun.*, vol. 64, no. 2, pp. 654667, Feb. 2016.

[31] Tim Schenk. 2008. RF imperfections in high-rate wireless systems: Impact and digital compensation (1st. ed.). Springer Publishing Company, Incorporated.

[32] C. Studer, M. Wenk and A. Burg, "MIMO transmission with residual transmit-RF impairments," 2010 *International ITG Workshop on Smart Antennas (WSA)*, Bremen, 2010, pp. 189-196.

[33] B. E. Priyanto, T. B. Sorensen, O. K. Jensen, T. Larsen, T. Kolding and P. Mogensen, "Assessing and modeling the effect of RF impairments on UTRA LTE uplink performance," 2007 *IEEE 66th Vehicular Technology Conference*, Baltimore, MD, 2007, pp. 1213-1217.

[34] X. Li, M. Liu, C. Deng, D. Zhang, X. Gao, K. M. Rabie, R. Kharel, "Joint effects of residual hardware impairments and channel estimation errors on SWIPT assisted cooperative NOMA networks," *IEEE Access*, vol. 7, pp. 135499-135513, Oct. 2019.

[35] E. Bjrnson, A. Papadogiannis, M. Matthaiou and M. Debbah, "On the impact of transceiver impairments on af relaying," 2013 *IEEE International Conference on Acoustics, Speech and Signal Processing*, Vancouver, BC, 2013, pp. 4948-4952.

[36] C. E. Shannon, "A mathematical theory of communication," *Bell System Technical Journal*, vol. 27, pp. 379-423 and 623-656, Jul. and Oct. 1948.

[37] B. Makki, T. Svensson and M. Zorzi, "Finite block-length analysis of the incremental redundancy HARQ," *IEEE Wireless Commun. Lett.*, vol. 3, no. 5, pp. 529-532, Oct. 2014.

[38] X. Lai, Q. Zhang and J. Qin, "Cooperative NOMA short-packet communications in flat Rayleigh fading channels," *IEEE Trans. Veh. Technol*, vol. 68, no. 6, pp. 6182-6186, June 2019.

[39] M. M. Molu, P. Xiao, M. Khalily, L. Zhang and R. Tafazolli, "A novel equivalent definition of modified Bessel functions for performance analysis of multi-hop wireless communication systems," *IEEE Access*, vol. 5, pp. 7594-7605, May 2017.

[40] L. Comtet, Advanced Combinatorics: The art of finite and infinite expansions. Amsterdam, The Netherlands: Reidel, 1974.

[41] A. K. Mishra, S. K. Tiwari, S. C. M. Gowda and P. Singh, "Performance analysis of bidirectional multi-user multi-relay transmission systems with channel estimation error and hardware impairment," *IEEE Trans. Veh. Technol.*, vol. 68, no. 9, pp. 8804-8813, Sept. 2019.

[42] M. Letafati, A. Kuhestani, H. Behroozi and D. W. K. Ng, "Jamming-resilient frequency hopping-aided secure communication for Internet-of-Things in the presence of an untrusted relay," *IEEE Trans. Wireless Commun.*, doi: 10.1109/TWC.2020.3006012.

[43] S. Xiao, Y. Guo, K. Huang and L. Jin, "High-rate secret key generation aided by multiple relays for Internet of things," *Elec. Lett.*, vol. 53, no. 17, pp. 1198–1200, Aug. 2017.

[44] R. C. Cannizzaro, P. Banelli and G. Leus, "Adaptive channel estimation for OFDM systems with doppler spread," 2006 *IEEE 7th Workshop on Signal Process. Advances in Wireless Commun.*, Cannes, 2006, pp. 1-5.

[45] Gradshteyn, I. S., Ryzhik, I. M. (1996), Table of integrals, series, and products , Elsevier/Academic Press, Amsterdam .

[46] M. Abramowitz. 1972. Handbook of mathematical functions, with formulas, graphs, and mathematical tables,. Dover Publications, Inc., USA.